Supercontinuum Generation in Speciality Optical Fibers: Design and Analysis

A Dissertation submitted towards the partial fulfilment of the requirement for the award of degree of

Master of Technology in
Microwave and Optical Communication Engineering

Submitted by
AGN Chaitanya
2K14/MOC/21

Under the supervision of
Dr. Ajeet Kumar
Assistant Professor

Department of Applied Physics and Department of Electronics & Communication Engineering

Delhi Technological University
(Formerly Delhi College of Engineering)

JUNE 2016

DELHI TECHNOLOGICAL UNIVERSITY

Established by Govt. of Delhi vide Act 6 of 2009
(*Formerly Delhi College of Engineering)*
SHAHBAD DAULATPUR, BAWANA ROAD, DELHI-110042

CERTFICATE

This is to certify that the work which is being presented in the dissertation entitled

"**Supercontinuum Generation in Speciality Optical Fibers: Design and Analysis**" is the authentic work of **A.G.N Chaitanya** under my guidance and supervision in the partial fulfilment of requirement towards the degree of Master of Technology in Microwave and Optical Communication Engineering jointly run by Department of Applied Physics and Department of Electronics and Communication in Delhi Technological University during the 2014-16.

As per the candidate declaration this work has not been submitted elsewhere for the award of any other degree.

Dr. Ajeet Kumar
Assistant Professor
Department of Applied Physics
DTU

Prof. P.R. Chadha
Professor
Head of Department
Electronics and Communication
DTU

Prof. S.C. Sharma
Professor
Head of Department
Applied Physics
DTU

DECLARATION

I hereby declare that all the information in this document has been obtained and presented in accordance with academic rules and ethical conduct. This report is my own, unaided work. I have fully cited and referenced all material and results, that are not original to this work. It is being submitted for the degree of Master of Technology in Microwave and Optical Communication Engineering at Delhi Technological University. It has not been submitted for any degree or examination in any other university.

A.G.N Chaitanya
M. Tech, MOCE
2K14/MOC/21

ABSTRACT

Optic fiber communication is the transmission of light as signal through an optically transparent medium which acts as channel by the principle of total internal reflection. The channel is a dielectric cylindrical waveguide of silica. The area in which the light travels is called core. Initially LED's were used as light source which were having low intensity and low coherence.

After invention of laser light for optical transmission through optical fiber, the phenomenon of nonlinear effects were discovered. The input-output power relation was no more linear and certain losses were observed and the losses increased with increase in input power. Investigation revealed that the high intensity optical light will give rise to certain nonlinear effects. This was due to response of the dielectric material to high intensity electromagnetic field. The polarization induced by electric dipoles is not linear to electric field.

The nonlinear effect give rise to two important effects called Kerr effect which is second order nonlinearity and third order nonlinearity called Pockel effect. These effects have resulted in many phenomenon such as Cross-phase modulation, Self-phase modulation, Stimulated Raman Scattering, Four wave mixing etc. The effect is dependent on material and geometry of the fiber.

Super Continuum Generation or SCG is a process that is a result due to interplay between linear and nonlinear effects. It is a process where a continuous spectrum of light is generated when a high intensity short duration laser pulse is propagated through a highly non-linear fiber. The resultant spectrum will have low temporal coherence (high bandwidth) and high spatial coherence.

The project involves design and analysis of supercontinuum generation of speciality optical fibers. SCG have been simulated in co-axial multicore silica and tellurite fibers using RP Fiber power software. SCG has also been simulated in a $Ge_{11.5}As_{24}Se_{64.5}$ Chalcogenide glass graded index photonic crystal fiber using vectorial finite element based COMSOL Multiphysics and MATLAB.

Silica has a very low nonlinear refractive index. Silica based optical fibers display very low nonlinear coefficient. Higher optical power and longer length fiber are required for SCG. Tellurite has ten times higher nonlinear refractive index compared to silica. SCG can be achieved at low pulse power with smaller length cable. The step index fibers have very large effective area which is an undesirable feature for nonlinear application. Dispersion engineering in these fibers are difficult.

PCF's offer very small effective mode area. Dispersion characteristics can be modified as per requirement by arranging the air holes. Chalcogenide fibers have very high nonlinear coefficient and is transparent in near-IR and mid-IR region. Graded index assists in achieving a better dispersion profile. Hence a chalcogenide glass graded index PCF has been designed for generation an ultra broadband continuum at near-IR and mid-IR region with a low peak power.

Such ultra-broadband supercontinuum spectrum is expected to have profound applications in various fields. The specific applications of mid-IR supercontinuum generation include spectroscopy, optical coherence tomography, frequency comb generation, early cancer detection, food quality control, security and sensing.

LIST OF RESEARCH PRESENTATION AND PUBLICATIONS

Publications:

1. AGN Chaitanya, Than Singh Saini, Ajeet Kumar, Ravindra Kumar Sinha **"**Supercontinuum Generation in co-axial multicore Silica fiber : Design and Analysis", Optik-International journal for Light and Electron Optics (Communicated –June 2016).

2. AGN Chaitanya, Than Singh Saini, Ajeet Kumar, Ravindra Kumar Sinha "Ultra broadband mid-IR Supercontinuum generation in $Ge_{11.5}$ $As_{24}Se_{64.5}$ based Chalcogenide graded index Photonic Crystal Fiber : Design and Analysis", Journal of Applied Optics (Communicated-June 2016)

Conference

1. AGN Chaitanya, Than Singh Saini, Ajeet Kumar "Dispersion Engineered $Ge_{11.5}$ $As_{24}Se_{64.5}$ based Graded Index Photonic Crystal Fiber for Nonlinear application" Conf proceeding, OSA Young Student Congress, 16-17 April 2016, MNIT Jaipur, Rajasthan, OSA_YSC_103, 7-10.

ACKNOWLEDGEMENT

The thesis work is a result of hard work and contribution of many well wishers, whose support and guidance has resulted in timely completion of project.

I would like to express my deepest gratitude to my supervisor **Dr. Ajeet Kumar**, Asst Professor, Department of Applied Physics. who accepted request of being my guide and for his invaluable support, quality guidance, priceless knowledge and constant motivation throughout the period of the project that has helped in timely completion and submission of this thesis.

I am deeply grateful to **Prof. S.C. Sharma**, H.O.D (Dept of A.P.), **Prof. Prem R. Chadha**, H.O.D (Dept. of ECE), **Prof R.K. Sinha**, **Prof. Rajiv Kapoor**, **Dr. Yogita Kalra** for their support, and also for providing us with all the facilities to carry out quality project work.

I would like to thank Dr. Than Singh Saini, research scholar for his valuable time and interest in the project. His knowledge, advice and time bound solutions for the queries raised during the course of the project have helped me in timely completion of the project work.

I also wish to express my heart full thanks to the classmates as well as staff at Department of Applied Physics and Department of Electronics and Communication of Delhi Technological University for their goodwill and support that helped me a lot, in successful completion of this project.

Finally, I want to thank my parents, for inculcating good ethos, as a result of which I am able to do my post-graduation from such an esteemed institution. I thank my wife for her silent support without which timely completion of the project work would not have been possible. I would thank my friends for believing in my abilities and for always showering their invaluable support and constant encouragement.

AGN Chaitanya
M.Tech. MOCE
2K14/MOCE/21

TABLE OF CONTENTS

LIST OF FIGURES

List of Tables

Chapter 1

Introduction

1.1 Thesis Approach:

The thesis consists of Supercontinuum Generation (SCG) in speciality optical fibers viz. co-axial multi-core step index and Photonic Crystal Fiber (PCF). Supercontinuum (SC) refers to broadening of an ultra-short high power optical pulse through a nonlinear fiber/waveguide of adequate length. The SC phenomenon is analysed using a multi-core co-axial step index silica and tellurite fiber using 'RP Fiber Power' software in the visible light region. The SC phenomenon in a $Ge_{11.5}As_{24}Se_{64.5}$ based Chalcogenide glass PCF is analysed using 'COMSOL-Multiphysics' software in near-IR and mid-IR region. RP Fiber Power solves the mode equation for calculating number of modes and split-step fourier method to solve nonlinear Schrödinger wave equation (NLSE). COMSOL-Multiphysics uses finite element method (FEM) for obtaining solutions. The analysis has been carried out for fundamental mode. The NLSE has been solved using MATLAB. Solution of NLSE is SCG. The effect of pulse power, pulse width and length of fiber on SC been investigated in all the three types of fibers.

1.2 Thesis Objectives:

The main objectives of the thesis are as follows:

- Study the basic properties of fiber and PCF such as dispersion, effective-mode-area, confinement loss, nonlinear coefficient.
- Study and understand the various nonlinear phenomenon like self-phase modulation (SPM), cross phase modulation (CPM), Four wave mixing (FWM), stimulated Raman scattering (SRS).
- Study the various numerical techniques involved in solving electromagnetic field problems like finite element method, finite difference method, and transfer matrix method.
- Design of co-axial multicore step index fiber (for silica and tellurite) for zero dispersion at pump wavelength and generate continuum in visible region using RP fiber power.

- Design of PCF for zero dispersion at pump wavelength and obtain effective mode index at pump wavelength using COMSOL-Multiphysics software. Using these values dispersion parameters are obtained and continuum is generated using MATLAB.
- Study the effects of various parameters like pulse width, pump power and length of the fiber on the broadening of the SCG.

1.3 Thesis Organisation:

The entire results of this project work has been organised into eight chapters. Chapter 1 gives a brief insight into the objectives of the thesis. Chapter 2 introduces optic fibers, PCF and various nonlinear effects that are responsible for the SCG. Chapter 3 is a brief description of nonlinear Schrodinger wave equation (NLSE), also various factors which effect SCG are discussed in detail. Chapter 4 gives an insight into various software for carrying out simulation in optical and opto-electrical domain and numerical techniques which are used for solving EM fields. In chapter 5 SCG in visible region has been simulated using a silica based co-axial multi-core step index fiber. The influence of pulse energy, pulse width and fiber length on spectrum broadening has been investigated. Chapter 6 describes the simulation of SCG in co-axial multicore step index tellurite fiber. Similar study on factors effecting spectral broadening as mentioned in previous chapter has been carried out. Chapter 7 is dedicated to supercontinuum generation in Chalcogenide glass graded index PCF. Conclusions are drawn in chapter 8, with brief details on scope for improvement of the present design.

Chapter 2

Optic Fibers and Nonlinear Effects

2. 1 Introduction:

An Optical Fiber is dielectric waveguide that guides the light through the phenomenon of total internal reflection. An Optical Fiber consists of

2.1.1 Core:

It is a doped silica or any other dielectric material (same as that of clad) which has a refractive index n_1 that is higher than that of cladding [1]. The light is guided inside the core through total internal reflection. A schematic representation of the structure is shown in Fig 2.1. The difference in refractive index between core and cladding Δn will be small.

2.1.1 Cladding:

It is either made of silica or any other material which is transparent to light and has refractive index n_2 lesser than that of core.

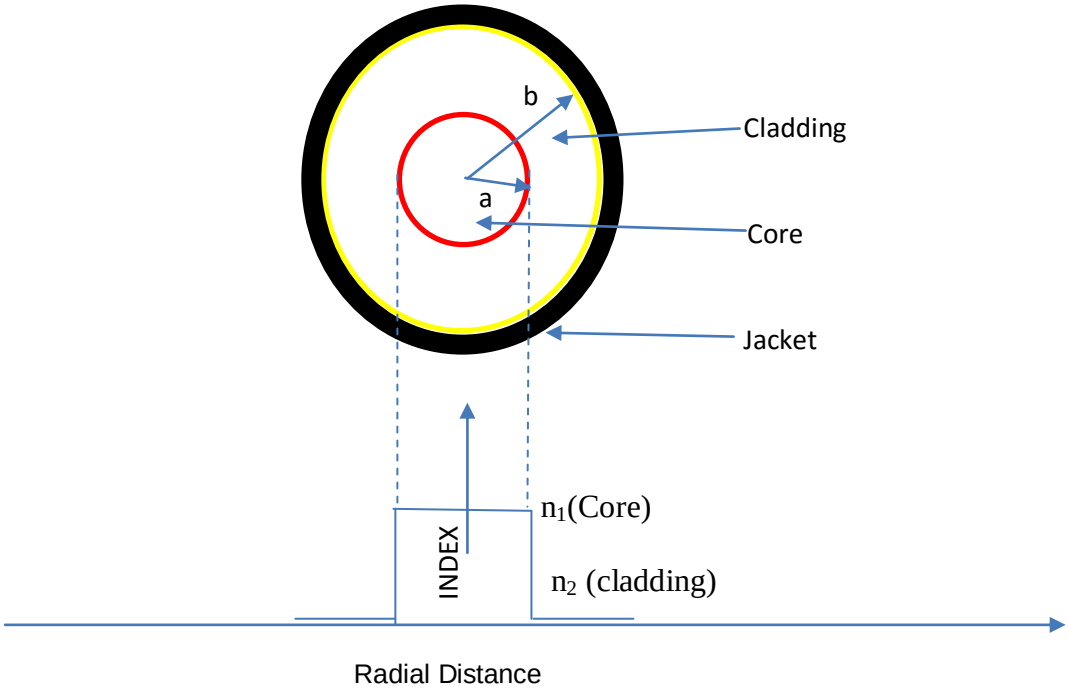

Fig 2.1 *Schematic Diagram of a step index fiber along with refractive index profile.*

The conventional step index fibers are not suitable for supercontinuum generation due to two main reasons

(a) Large effective mode area.

(b) Dispersion engineering in these fibers are difficult.

2.2 Photonic Crystal Fibers:

Photonic Crystal Fibers (PCF) are a new class of fibers invented by Knight and Russel in 1996 [2]. It is also known as microstructure fibers. It contains a fine array of air holes running parallel to the axis of the fiber that acts as cladding. The PCF may even contain array of another material.

Due to the presence of air holes the area around the axis acts as core due to relatively higher refractive index. The effective refractive index in and around the cladding area is due to that of combination of both air and the fiber material. The guided modes can be trapped in the central region of the PCF (core) due to higher average index that the cladding containing the air holes. The guidance will be due to total internal reflection (TIR). The core of the PCF will have a higher refractive index compared to cladding. The refractive index profile is shown in Fig 2.2 (a).This type of guidance is called index guidance.

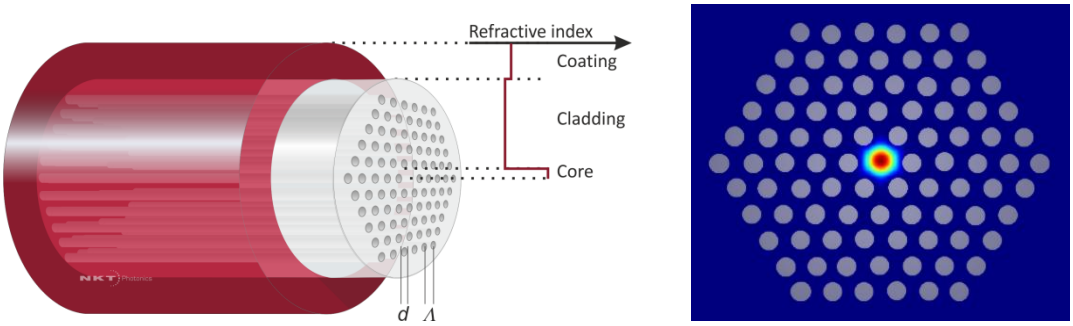

(a) (b)

Fig. 2.2 (a) Index guiding PCF (side view) , (b) Index guidance PCF (fundamental mode) (Courtesy: NKT Photonics website).

Another type of guidance is the photonic band gap guidance [3]. In this type, the guidance of light is based on photonic band gap which allows light to propagate in a hollow core region or a low index region as shown in Fig 2.3 (a) and Fig 2.3 (b). The fibers having such type of guidance have low nonlinearity and have very narrow pass-band approx. 100-200 nm. The PCF can be fabricated by stack and draw technique or by extrusion [4]. Such fibers can be designed to have extremely small mode areas such that they can be employed for nonlinear applications. Since the effective index and mode area depends on the arrangement of the air

holes the dispersion characteristics and effective mode area can be controlled as per the requirement of the design

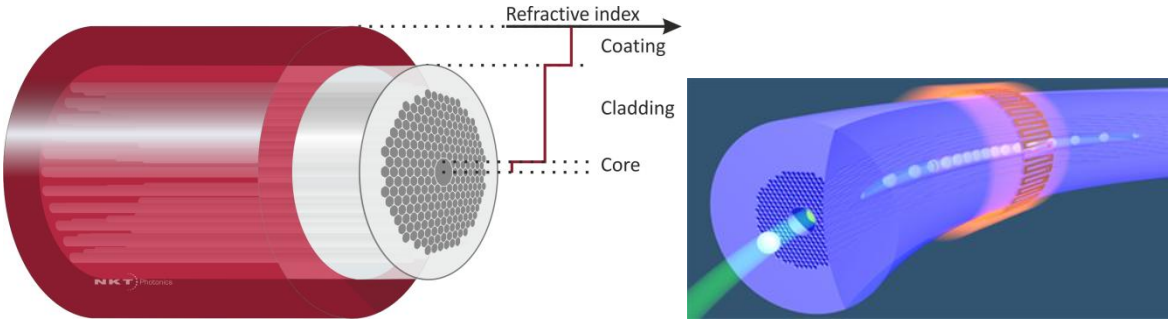

Fig 2.3 *(a) Band gap guidance PCF (side view) , (b) Band gap guidance PCF (fundamental mode). (Courtesy: NKT Photonics Website)*

. PCF's have been used to realise various components such as cavity fiber laser [5], long periodic fiber gratings [6], fiber amplifiers [7], power splitters [8], wavelength converters [9], wavelength demultiplexers [10], add-drop filters [11].

2.3 Nonlinear Effects:

In fiber optics the terms linear and nonlinear phenomenon can expressed as power independent or power dependent phenomenon respectively [12]. Nonlinear phenomenon in fiber optics occurs due to

(a) Dependence of refractive index on intensity

(b) Inelastic-scattering phenomenon.

Nonlinear phenomenon occur at high power level and is independent of wavelength. Till the threshold power, the graph input-output follow linear relation. Beyond threshold power, nonlinear phenomenon occurs and power input-output will no more have linear relation as shown in Fig 2.4.

At high power the total polarization **P** induced by the electric dipoles is not linear in the electric field, but can be expressed as power series in the field strength **E** as [13]

$$P = \epsilon_0 [\chi^{(1)} E + \chi^{(2)} E^2 + \chi^{(3)} E^3 \ldots\ldots] \quad (2.1)$$

The quantities $\chi^{(2)}$ and $\chi^{(3)}$ are known as second and third order nonlinear susceptibilities. If the higher order susceptibilities are absent then

$$P = \epsilon_0 \chi^{(1)} \mathbf{E} \quad (2.2)$$

represents the linear behaviour of induced polarization with respect to electric field.

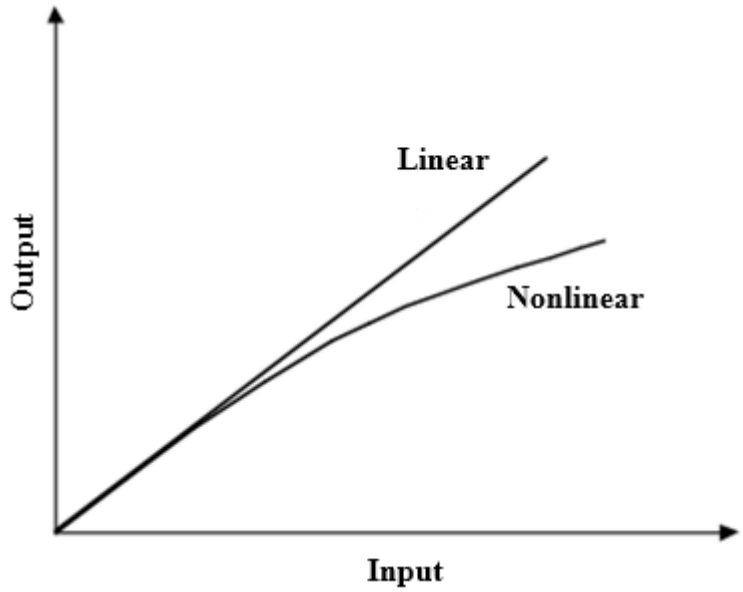

Fig 2.4. Graph with linear and nonlinear input-output relationship

The power dependence of the refractive index is responsible for the Kerr-effect. Depending upon the type of input signal, the Kerr-nonlinearity establishes itself in three different effects such as Self-Phase Modulation (SPM), Cross-Phase Modulation (CPM) and Four-Wave Mixing (FWM). In this phenomenon no energy is exchanged between the electromagnetic field and the dielectric medium. If the applied optical power is beyond certain threshold, the intensity of scattered light grows exponentially resulting in inelastic scattering phenomenon. In this, the optical field transfers part of its energy to the nonlinear medium. The two important effects under this category are Stimulated Brillouin-Scattering (SBS) and Stimulated Raman-Scattering (SRS). In Raman scattering incoherent optical phonon without any macroscopic wave is generated. In Brillouin scattering coherent acoustic phonon result in a macroscopic acoustic wave in the medium.

In Eqn 2.1 second order susceptibility $\chi^{(2)}$ is responsible for second harmonic generation and sum-frequency generation. Any medium in which inversion symmetry is absent, second order nonlinear effects doesn't exist. The lower order nonlinear effects are the third order nonlinear effects in fibers [14]. In most of the materials second order nonlinearity is absent, and only third order nonlinearity is considered.

2.3.1 Self-Phase Modulation (SPM):

The phase shift φ introduced by an electric field E over a fiber length L is given by

$$\varphi_L = \frac{2\pi}{\lambda} nL \tag{2.3}$$

The dependence of the refractive index on optical intensity causes a nonlinear phase shift while propagating through an optical fiber. The total phase shift is given by

$$\varphi_T = \frac{2\pi}{\lambda}(n_1 + n_2 I)L_{eff} \tag{2.4}$$

where, λ is the wavelength of the optical wave, I is the intensity of the optical field and L/L_{eff} is the propagation distance. The second term is the nonlinear phase shift φ_{NL} which is intensity dependent.

When a Gaussian or a secant hyperbolic (sech) pulse is coupled to a fiber with small core area, the higher intensity region of the pulse experiences the optical medium with higher refractive index whereas the lower intensity portions experience the same optical medium as lower refractive index as it propagates through the fiber. This time varying signal intensity will lead to a time varying refractive index, with the leading edge of the high intensity pulse experiencing a positive refractive index and the trailing edge of the same pulse experiencing a negative refractive index as shown in Fig. 2.5. This temporally varying refractive index will lead to a temporally varying phase change. The optical phase changes with time in exactly the same way as optical signal [15]. Since the modulation is self-induced, it's called as self-phase modulation (SPM).

Since the intensity of pulse gradually varies with time, the pulse will undergo different phase shift. This results in frequency chirp with the rising edge of the pulse experiencing frequency shift in the upper side and the trailing edge experiences the frequency shift on the lower. This leads to the spectral broadening of the pulse [16].

In case of self-phase modulation there will be broadening of spectrum without any change in temporal distribution, i.e. the pulse width remains preserved but its contents will change. In case of dispersion the broadening of pulse occurs in time domain and spectral contents are unaltered.

.

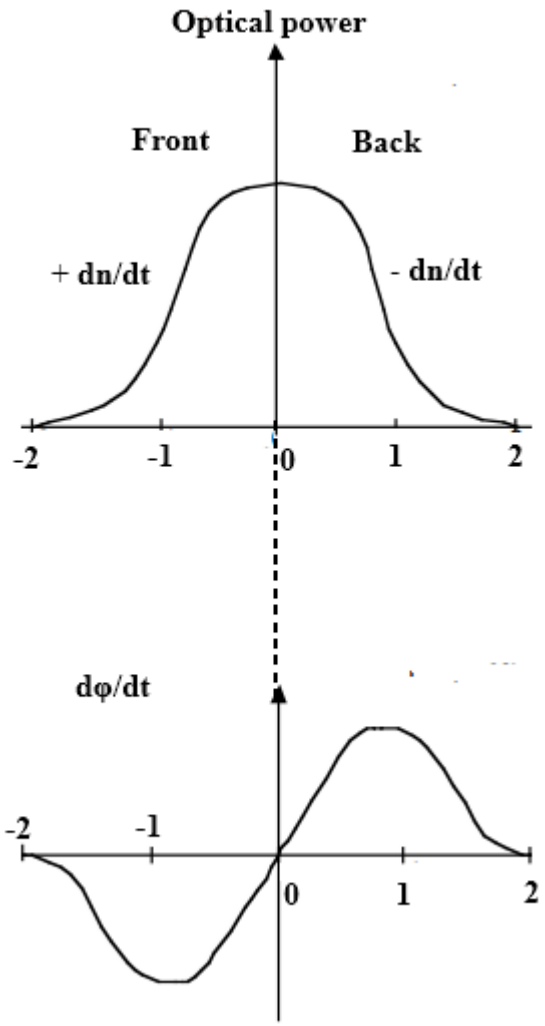

Fig 2.5. Self-Phase Modulation
(Courtesy: S.P. Singh and N. Singh 'Nonlinear Effects in Optical Fibers: Origin, Management and Applications' PIER)

2.3.2 Cross Phase Modulation (CPM):

Cross Phase Modulation of CPM occurs when two or more optical fields simultaneously propagates inside optical fibers, they interact with each other through nonlinear dielectric medium or fiber. CPM is always accompanied by SPM. This occurs because the nonlinear refractive index seen by an optical field depends not only on the intensity of that beam, but also on the intensity of co-propagating beams [17]. CPM results in asymmetric spectral broadening. The pulse shape is distorted in CPM.

CPM occurs in multichannel system. In multichannel system, the nonlinear phase shift of the signal around central wavelength λ_i is given by

$$\varphi_{NL} = \frac{2\pi}{\lambda} n_2 L[I_i(t) + 2\sum_{i \neq j} I_j(t)] \quad (2.5)$$

In the above equation the first term is responsible for SPM and the second term is CPM. The second term is multiplied by a factor which indicates that CPM is effective by a factor of two compared to SPM for the same amount of power and other associated conditions. The factor 2 in the second term has its origin in the form of nonlinear susceptibility [14]. Such interactions can generate new waves under appropriate conditions through nonlinear process such as SRS or SBS. The Kerr-type nonlinear effect can also couple two optical field through CPM without any energy transfer between them. CPM is a major drawback in DWDM systems since it converts power variations or fluctuations in a particular channel to phase fluctuation in other co-propagating channels. This may lead to asymmetric spectral widening or broadening and also pulse getting distorted.

2.3.3 Four-Wave Mixing (FWM):

It is a parametric process and is classified as third order susceptibility $\chi^{(3)}$. The third order parametric process involve nonlinear interaction between four optical waves and include process such as third harmonic generation, four wave mixing and parametric amplification [18-21]. The third-order parametric process involves nonlinear interaction among four optical waves and include phenomenon such as four wave mixing or third-harmonic generation. If three optical fields of frequencies ω_1, ω_2 and ω_3 simultaneously propagate inside a nonlinear dielectric medium or fiber it generates a fourth field of frequency ω_4. The newly generated frequency will be related to the original three frequencies by

$$\boldsymbol{\omega_4 = \omega_1 \pm \omega_2 \pm \omega_3} \quad (2.6)$$

as shown in Fig 2.6. In this the new frequency that is generated lies between ω_1 and ω_2. The power of the newly generated wave is lesser compared to that of the original three waves. The total energy is conserved in this process. This process is very sensitive and requires phase matching condition to be satisfied. Dispersion plays an important role in this process. The process results in symmetrical broadening of the pulse.

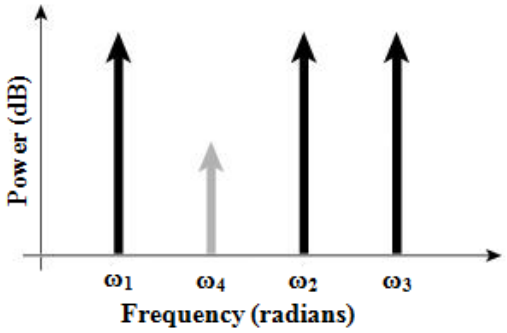

Fig. 2.6 Four Wave Mixing

Relating the above phenomenon in quantum-mechanical context, FWM occurs when photons from one or more wave are annihilated or destroyed and new photons of different energy are created i.e. these photons will be of different frequencies which may be of the combination of any of the above frequency combination of ω_1, ω_2 and ω_3. The important thing is to note that the new photons that are created at different frequencies are such that net energy and momentum are conserved during the interaction between frequencies. In FWM the EM waves generating in a fiber generate new waves [22]. FWM is similar to inter-modulation distortion in electrical systems.

2.3.3 Raman Scattering (RS):

The Raman scattering effect is the inelastic scattering [13] of a photon with an optical phonon, which originates from a finite response time of the third order nonlinear polarization [23] of the material

Stimulated Raman Scattering (SRS) is an inelastic scattering phenomenon in which transfer of energy takes place between optical fields simultaneously propagating in a dielectric medium or a nonlinear fiber [24]. The result of this transfer results in down shift of frequency determined by vibrational modes of the dielectric medium [25]. The energy transfer is of the order of 10^{-6}. These processes were discovered by Sir C.V. Raman and hence know as Raman Effect. Raman scattering has been used to convert an optical fiber into broadband Raman amplifier, tunable Raman lasers etc. This phenomenon occurs only when the power exceeds threshold power (P_r) given by [1]

$$P_r = 5.9 * 10^{-2} * d^2 * \lambda * \alpha_{dB} \text{ watts} \quad (2.7)$$

Where d is diameter of fiber in μm

λ is wavelength in μm

α_{dB} is attenuation of fiber in dB/Km

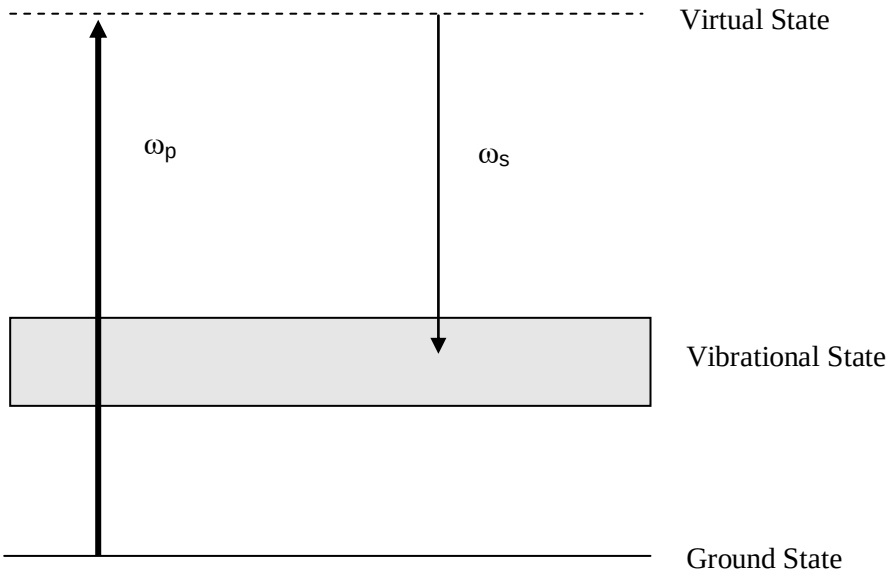

Fig 2.7 Schematic illustration of Raman Scattering from a quantum mechanical view point

In context of quantum-mechanics the phenomenon is may be described as conversion of a photon of energy $h\omega_p$ by a molecule to a lower frequency photon with energy $h\omega_s$ as the molecule makes transition to a vibrational excited state as shown in Fig 2.7. The nonlinear phenomenon of SRS can occur in which Stokes wave (long wavelength) grow rapidly inside the medium such that most of the pump energy is transferred to it.

Raman Scattering can occur both in forward and backward direction. Raman scattering leads to stokes scattering where energy of resultant photon reduces or increase in wavelength is observed or anti-stokes scattering where energy of resultant photon due to molecular vibration increases resulting in a lower wavelength light. The anti-stokes scattering is weaker than stokes scattering and are temperature dependent [26].

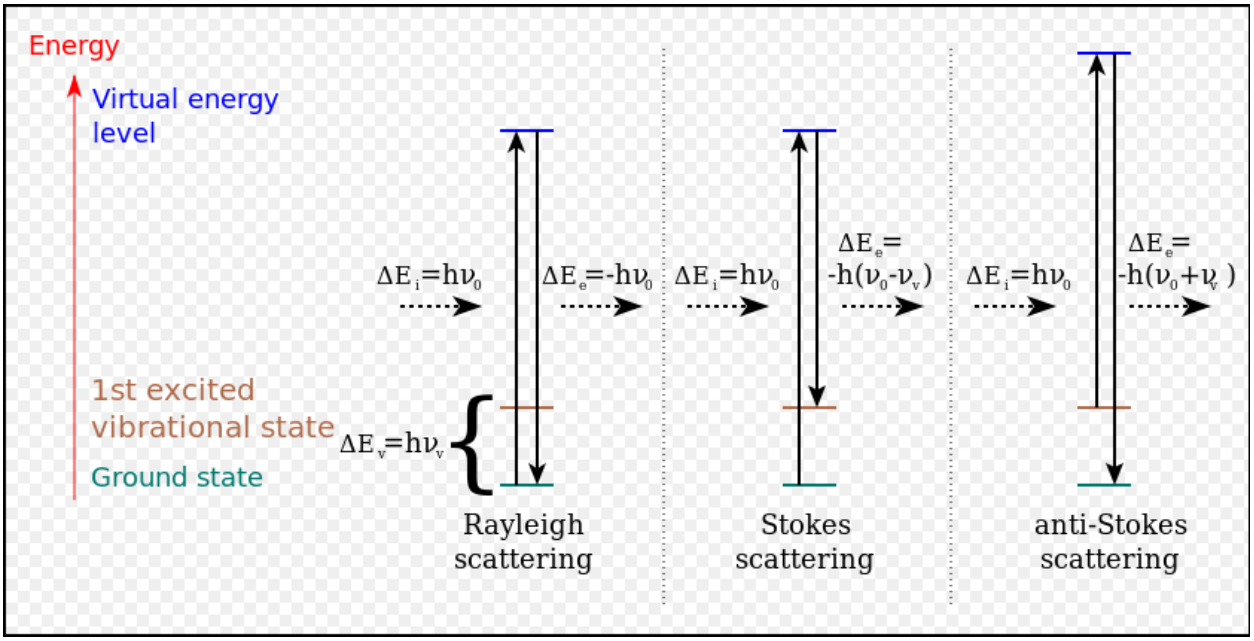

Fig. 2.8. Different possibilities of light scattering Rayleigh scattering, stokes Raman Scattering and Anti Stokes Raman Scattering.
(Courtesy: Wikipedia)

RS occurs at higher power three orders of magnitude compared to SBS. The phenomenon is depicted in Fig 2.8

2.3.5 Self-Steepening Effect.

Self-steepening results from intensity dependence of group velocity [27]. It leads to asymmetric broadened spectra of ultra-short pulses. As the pulse propagates inside the fiber it becomes asymmetric with its peak shifting towards the trailing edge. This results in a steeper trailing edge as the pulse propagates. Physically the group velocity is intensity dependent such that the peak move at lower speed that the wings or edges. Self-steepening creates optical shock which is similar to acoustic shock on the leading edge. At higher power and for pulses less than 100 fs the self-steepening effect can occur at very short distance. The spectrum broadening is asymmetric with longer tail towards shorter wavelength. The self-steepening effect is shown in Fig 2.9

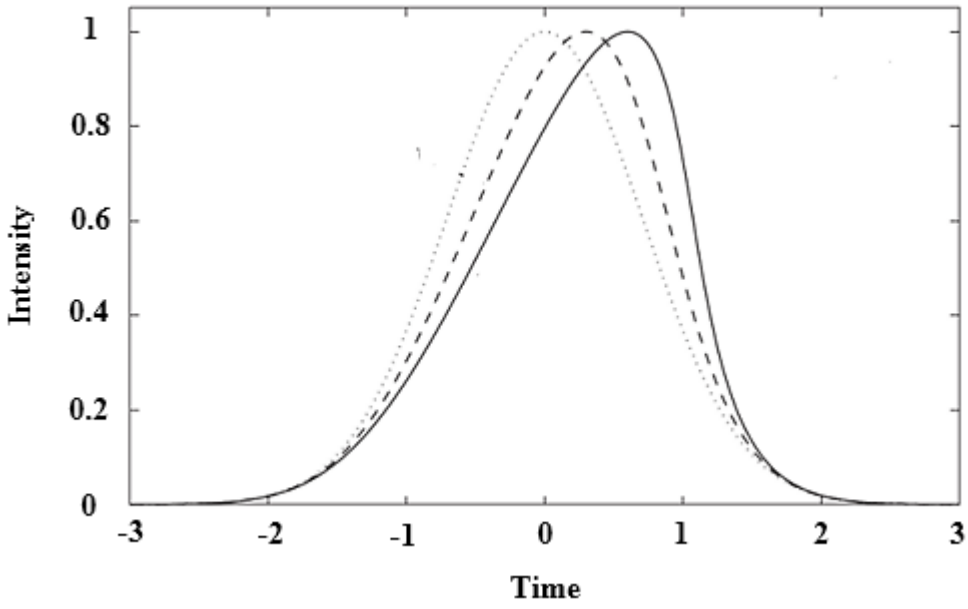

Fig 2.9. Self-Steepening of Gaussian Pulse when there is no dispersion.. The dotted line is the shape of the pulse at z=0
(Courtesy: Nonlinear optics by GP Agrawal)

Chapter 3

Nonlinear Schrödinger Wave Equation and Supercontinuum Generation

3.1 Introduction:

The NLSE is an example of a universal nonlinear model that describes many physical nonlinear systems. The equation can be applied to nonlinear acoustics, hydrodynamics, nonlinear optics, quantum condensates, heat pulses in solids and various other nonlinear instability phenomena.

The nonlinear effects discussed in the previous chapter are described numerically by nonlinear Schrodinger wave equation. The nonlinear Schrodinger wave equation is given by [14]

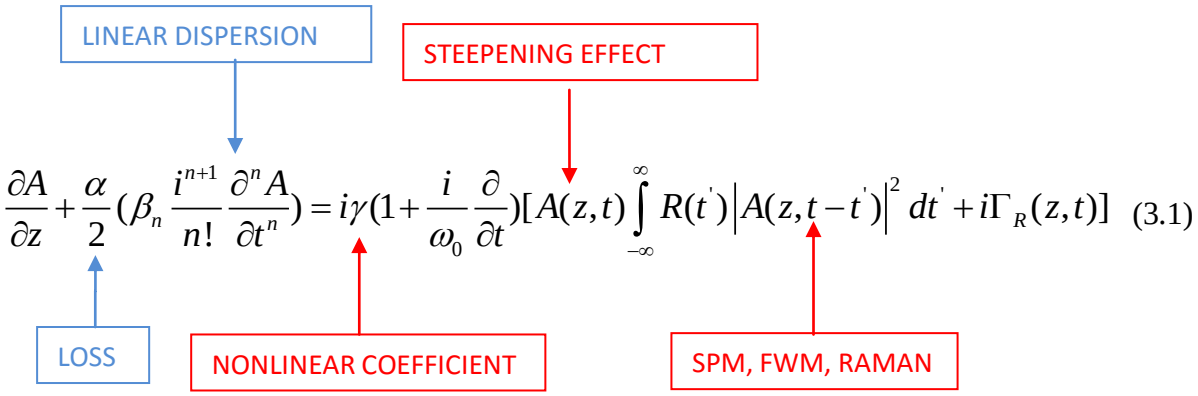

$$\frac{\partial A}{\partial z}+\frac{\alpha}{2}(\beta_n \frac{i^{n+1}}{n!}\frac{\partial^n A}{\partial t^n})=i\gamma(1+\frac{i}{\omega_0}\frac{\partial}{\partial t})[A(z,t)\int_{-\infty}^{\infty} R(t')\left|A(z,t-t')\right|^2 dt' + i\Gamma_R(z,t)] \quad (3.1)$$

The LHS of the NLSE describes the linear effects and the RHS of the equation describes the nonlinear effect. The supercontinuum generation is due to interplay of both linear and nonlinear effects as the pulse propagates. Supercontinuum generation can be numerically solved by solving NLSE.

To determine electric field distribution in a fiber or a waveguide several techniques have been developed. The techniques may be broadly classified as experimental, analytical and numerical. Experimental methods are costly, analytical methods are lengthy and require complex mathematical equations to be solved. Numerical methods are neither time consuming nor expensive and can be solved using computers. NLSE can be solved using

various numerical techniques [28-33]. The technique used to solve NLSE in the project is Split Step Fourier Method (SSFM).

3.2 Split Step Fourier Method:

SSFM is a pseudo-spectral numerical method to obtain solutions for partial differential equations like NLSE. This method is being extensively used to solve pulse propagation in nonlinear dispersive media [34, 35]. The name SSFM arises for two reasons

(a) The method computes solution in small steps and separately calculates the linear and nonlinear effects.

(b) Frequent Fourier transformation is carried out since the linear step is solved in frequency domain and the nonlinear step is solved in time domain.

This method is relatively faster compared to most of the finite difference schemes such as Crank–Nicolson method, Linearized Crank–Nicolson method, Du Fort-Frankel type, Besse relaxation scheme. This is due to the use of finite-Fourier-transform (FFT) algorithm [36]. In split step NLSE can be written in the form of

$$\frac{\partial A}{\partial z} = (\hat{D} + \hat{N})A \tag{3.2}$$

where, $\hat{D}$ is a differential operator that accounts for linear losses like dispersion and attenuation losses in a linear medium as depicted in the LHS of the NLSE. The $\hat{N}$ is a nonlinear operator that governs the effect of nonlinearities in fiber and A is the amplitude of the pulse. In this method the approximate solution is obtained by assuming that nonlinear and dispersive effects act independently as the optical field propagates over a small distance h. Therefore, as the field propagates from z to z+h, the NLSE can be solved by initially assuming nonlinearity acts alone i.e. $\hat{D}$=0 and subsequently dispersion acts alone i.e.. $\hat{N}$ =0.

The implementation of split-step Fourier method is relatively straight forward. The fiber is divided in to large number of equal segments. The optical pulse is propagated from segment to segment. The field A (z,T) is first propagated for a distance of h/2 with dispersion only using FFT algorithm. At the middle of the segment z+h/2 the effect if nonlinearity is multiplied that represents the nonlinear effect for the whole segment of length h. For the next half of the segment only dispersion effect is calculated to obtain the solution for the

entire segment A(z+h,T). This method assumes nonlinearity to be lumped at the middle of the segment as shown in Fig 3.1.

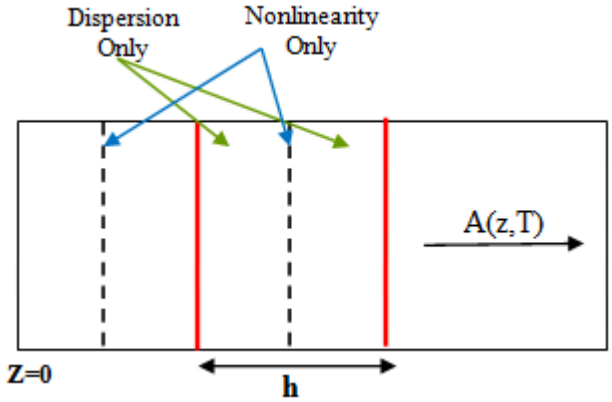

Fig. 3.1 Split step Fourier method

SSFM has limitation when large number of FFT operations has to be performed or when the temporal window is small. One such area is wavelength division multiplexing (WDM) in which the temporal resolution is about 50 fs and temporal window is about 1-10 ns. In such cases finite difference methods are employed**.**

3.3 Supercontinuum Generation:

Super continuum generation (SCG) is a process where laser light which has high temporal and spatial coherence [37] is converted to a light with low temporal coherence and high spatial coherence. A SC source provides an ultra-broad band spectrum, but with single mode beam characteristics and excellent pointing stability with brightness of a laser. The phenomenon was first observed by Dr. Alfano and Dr. Shapiro in 1970's [38, 39]. SCG is generated when a ultrashort pulse of high intensity is propagated through a highly nonlinear fiber/waveguide of adequate length as shown in Fig 3.2

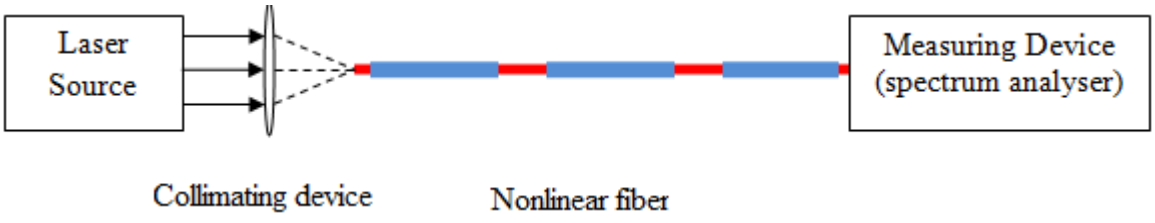

Fig. 3.2 Super continuum generation process diagram

The term SC does not cover a specific phenomenon but rather a plethora of nonlinear effects, which, in combination, lead to extreme pulse broadening. To achieve this following conditions are to be satisfied

(a) Short pulse of high intensity.

(b) Small Core Size.

(c) Normal Dispersion in the region of interest.

(d) Minimum Dispersion at pump wavelength.

(d) Adequate fiber length.

(e) High nonlinear refractive index of the medium.

3.3.1 Short pulse of high intensity:

When a high intensity short pulse as shown in Fig 3.3 is incident on a fiber with high nonlinear refractive index self-phase modulation occurs. The phenomenon of SPM alone cannot produce spectral broadening of more than 100 nm or more [14]. CPM is another mechanism that broadens the spectrum. The high intensity optical field is responsible for SRS. This mechanism creates stokes band and anti-stokes band. The SRS mechanism broadens the spectrum mainly on longer wavelength region (Stokes wave). FWM is another nonlinear effect that can broaden the continuum on either side provided phase matching condition is satisfied.

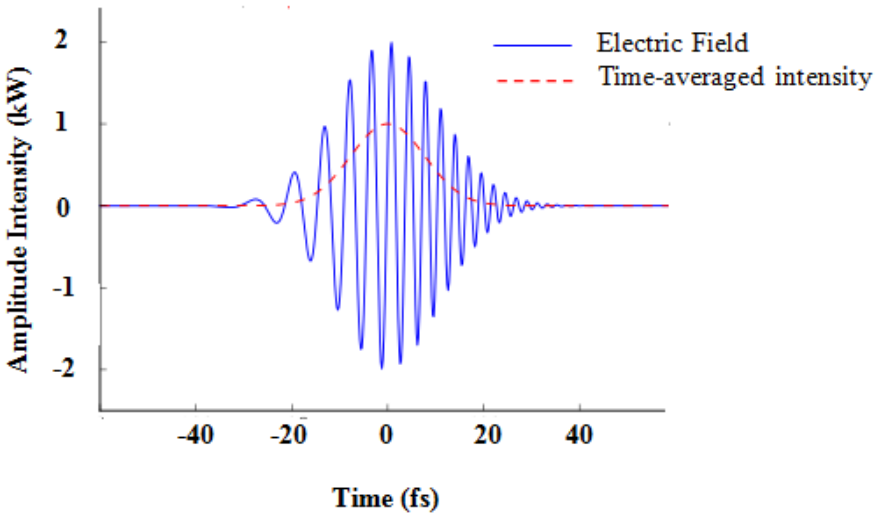

Fig 3.3 Short high intensity pulse

The role of FWM is highly dependent on dispersion characteristics of the fiber and plays a critical role in SCG. Since a large spectral width is generated during the process, the GVD or β_2 cannot be treated as constant over the entire spectral width. Its wavelength dependence

should be included through higher-order dispersion parameters. The SCG can be enhanced if dispersion varies along the fiber. The flatness of the continuum improves if β_2 increases along the fiber such that optical pulse experience anomalous GVD near the front end of the fiber and normal GVD close to the output end [40].

3.3.2. Small Core Size

The effect of nonlinearity grows with intensity in fiber and the intensity is inversely proportional to area of the core. From the NLSE the RHS is multiplied by a factor γ, which is the nonlinear coefficient. It is given by [14]

$$\gamma = 2\pi \frac{n_2}{A_{eff}\lambda} \quad \text{m}^{-1}\text{W}^{-1} \tag{3.3}$$

where, n_2 is nonlinear refractive index of medium in m^2/W

The term effective cross sectional area is used since the power is not uniformly distributed within the cross section of the fiber. The effective cross-sectional area (A_{eff}) is calculated using [14] as shown in Fig 3.4

$$A_{eff} = \frac{(\int_{-\infty}^{\infty}\int |E|^2 \, dxdy)^2}{(\int_{-\infty}^{\infty}\int |E|^4 \, dxdy)} \quad \text{m}^2 \tag{3.4}$$

For nonlinear application such as SCG a high nonlinear coefficient is desired and hence γ is to be optimised. This can be carried out by fiber design reducing effective mode area (by increase index difference between core and cladding). A small cores size results in efficient nonlinear effect. The smaller core helps in effective interaction of fields resulting in generation of harmonics or new wavelengths.

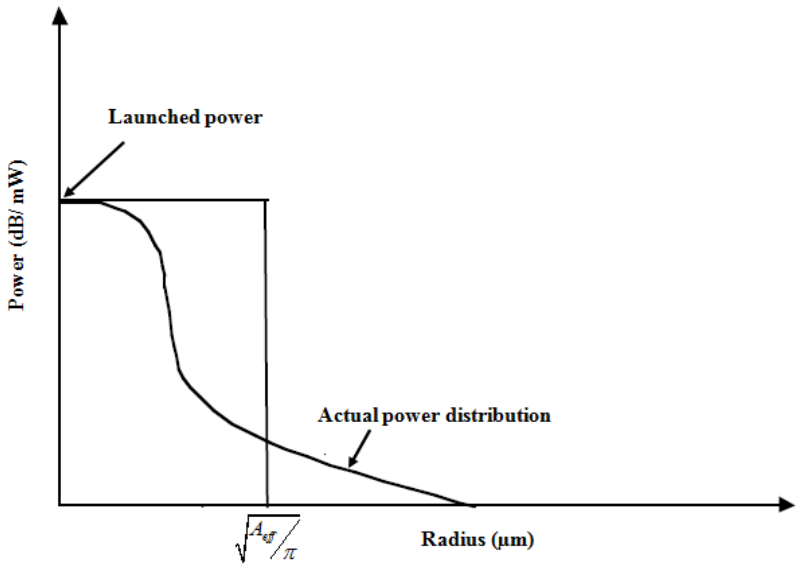

Fig 3.4 Definition of effective area.

3.3.3. Effect of Dispersion on SCG

Chromatic dispersion in an optical fiber refers to phenomenon where the phase velocity and group velocity of the pulse propagating depends on the frequency of the pulse. This arises since the source is nearly monochromatic. Chromatic dispersion of second order and higher order is defined via the Taylor series expansion in terms of wave number 'β' as a function of the angular frequency ω (radians) around the center frequency ω_0 [41] . The equation is given by

$$\beta(\omega) = \beta_0 + \frac{\partial\beta}{\partial\omega}(\omega-\omega_0) + \frac{1}{2}\frac{\partial^2\beta}{\partial\omega^2}(\omega-\omega_0)^2 + \frac{1}{6}\frac{\partial^3\beta}{\partial\omega^3}(\omega-\omega_0)^3 + ... \quad (3.5)$$

where,

β_0, is the zero order term and it describes common phase shift.

$\beta_1 = \frac{\partial\beta}{\partial\omega}$, is the first order term and contains inverse group velocity or the group delay per unit length and describes an overall time delay without an effect on shape pulse

$\beta_2 = \frac{\partial^2\beta}{\partial\omega^2}$, is the second order term second-order dispersion per unit length and describes an overall delay with an effect on shape of the pulse

$\beta_3 = \frac{\partial^3\beta}{\partial\omega^3}$, is the third order dispersion per unit length and is important in ultra-short pulses because of their wide bandwidth

Depending on the value of β_2 (GVD) either positive or negative the dispersion region can be divided into normal or anomalous dispersion region as shown in Fig 3.5

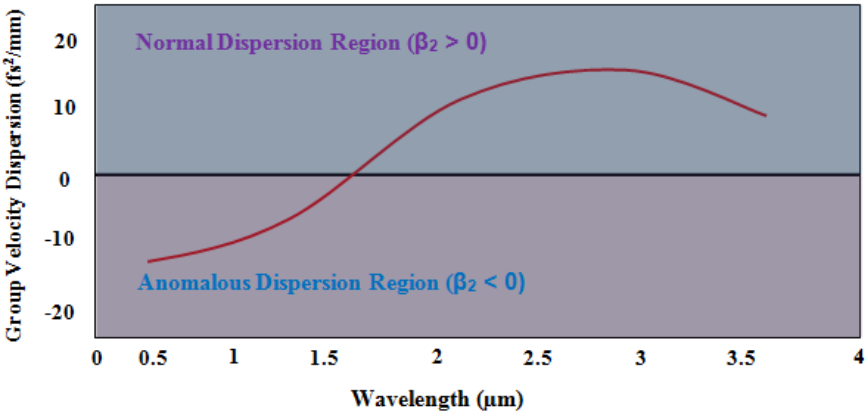

Fig.3.5 Normal and anomalous dispersion region

3.3.3.1 Normal dispersion region.

In normal dispersion region $\beta_2 > 0$ the group velocity decreases with increasing frequency i.e. higher frequency component (blue) travel slower compared to lower frequency component (red). This phenomenon helps in maintaining the pulse shape and hence SPM is dominant. SCG is very deterministic and the phase coherence of the supercontinuum pulses generated are very high even under the condition of strong spectral broadening. Therefore the pump wavelength should lie in the normal dispersion region and should be as low as possible.

3.3.3.2 Anomalous dispersion region

In anomalous dispersion region $\beta_2 < 0$ group velocity increases with increasing optical frequency i.e. lower frequency component (red) travel slower compared to higher frequency components (blue). SPM and dispersion effect will lead to formation of solitons due to modulation instability [42-44]. SPM generates frequency chirp such that it chirps leading edge with lower frequencies and trailing edge with higher frequencies. On the other hand dispersion in this region will negate the above effect and with choice of proper pulse shape, the pulse would propagate undistorted. A pulse which neither broadens in time domain nor in frequency domain is called solitons. Choosing a pump wavelength in anomalous dispersion region will involve soliton dynamics, including the split-up of higher-order solitons into multiple fundamental soliton (soliton fission). SCG process is sensitive to the

slightest fluctuations (including quantum noise). The properties of the spectrally broadened pulses vary substantially from pulse to pulse.

3.3.4 Zero dispersion at pump wavelength

Dispersion in fibers can be attributed due to material and waveguide geometry. Each material has a fixed zero dispersion wavelength (ZDWL). All materials have zero dispersion at certain wavelength. For *e.g.* Silica fibers exhibit zero dispersion at 1310 nm. The pump wavelength may not be coinciding with ZDWL of the material. In order to achieve zero dispersion at pump wavelength, the waveguide geometry is to be modified. Zero dispersion at pump wavelength preserves the shape of the pulse leading to an efficient generation of continuum. Distortion in pulse shape or pulse spreading will lead to loss of power, thus decreasing the pulse width.

3.3.5 Adequate Fiber Length

Depending on the initial width T_0 and peak power P_0 of the incident pulse, either dispersive or nonlinear effects may dominate along the fiber. There are two lengths: dispersion length L_D and the nonlinear length L_{NL} [14]. The dispersion length and nonlinear length are given by

$$L_D = \frac{T_0^2}{|\beta_2|} \quad \text{m} \qquad \text{3.6 (a)} \qquad\qquad L_{NL} = \frac{1}{\gamma P_0} \quad \text{m} \qquad \text{3.6 (b)}$$

If the fiber length L is such that, $L \ll L_{NL}$ and $L \ll L_D$, neither dispersive nor nonlinear effects play a significant role during pulse propagation. This condition is achieved when the pulse power is less, and GVD is minimum. This is the desired condition for telecommunication cables. As a result pulse maintain its shape during propagation through the fiber. If the fiber length is such that $L \ll L_{NL}$ but $L \sim L_D$ the pulse evolution is governed by GVD, and nonlinear effects play a minor role. If the fiber length L is such that $L \ll L_D$ and $L \sim L_{NL}$ the dispersion is negligible and pulse evolution in the fiber is governed by SPM that produces a change in pulse spectrum. This is the desired condition for SCG. If the fiber length L is larger than L_D and L_{NL} , dispersion and nonlinearity act together as pulse propagates. The interplay of GVD and SPM can be used for solitons generation in anomalous dispersion region or pulse compression in normal dispersion region

3.3.6. High nonlinear refractive index of the medium

The nonlinear effects in the optical fibers are initiated due to nonlinear refraction which a phenomenon due to intensity dependence of refractive index [45]. The refractive index can be written as

$$n(\omega,I) = n(\omega)+n_2 I \tag{3.7}$$

where, $n(\omega)$ is the linear part, I is the optical intensity and n_2 is the nonlinear refractive index associated with third order susceptibility. This intensity dependence of refractive index leads to nonlinear phenomenon in materials. This parameter is fixed for each glass material. A higher nonlinear refractive index will result in better nonlinear effects i.e. a broader spectrum with higher power.

3.3.7 Raman Response

Raman gain is the optical gain due to stimulated Raman scattering at high intensities. When analysed in the time domain, Raman gain has a simple physical interpretation. The application of a short, high-intensity optical pulse to a molecule disturbs the electronic structure of the molecule and results in an intensity dependent change in the polarisation of the molecule, or an intensity-dependent refractive index. The effect is shorter than the optical pulse. The optically induced perturbation in the electronic structure perturbs the field seen by the nuclei of the molecule [45]. This results in additional changes in polarisation associated with the excitation of molecular vibrations, and is called Raman effect. The vibrations of the molecule is the Raman response. Figure 3.6 (a) shows the experimentally measured Raman-gain spectrum and Fig 3.6 (b) the temporal form of $h_R(t)$ deduced from it [46].

If it is assumed that single vibrational frequency Ω_R, of the molecule is involved in the Raman process, $h_R(t)$ can be written in the form [16]

$$h\_R(t) = \frac{\tau_1^2 + \tau_2^2}{\tau_1^1 \tau_2^2} * \exp(-t/\tau_2) \times \sin(t/\tau_1) \tag{3.8}$$

where, $\tau_1 = 1/\Omega_R$ in femto-seconds

Ω_R, is the vibrational frequency of molecule

τ_2, is damping time of vibrations in femto-seconds

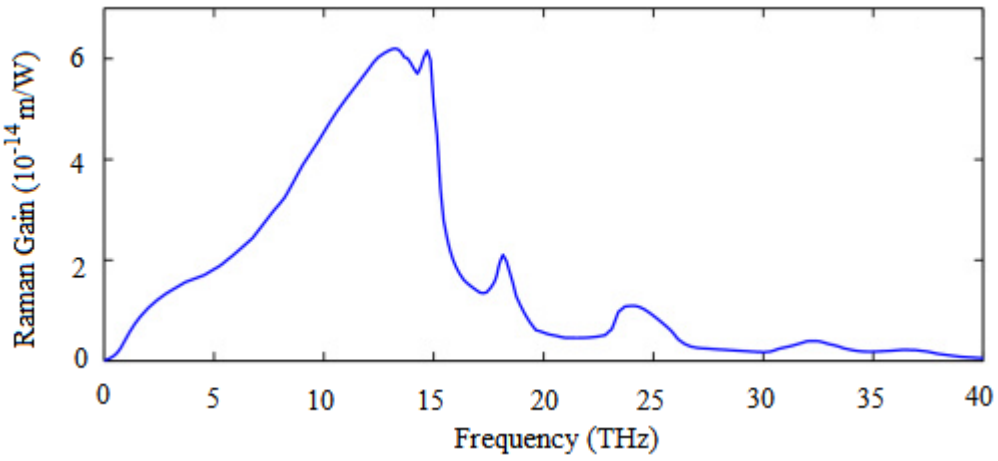

Fig 3.6 (a) Raman gain spectrum

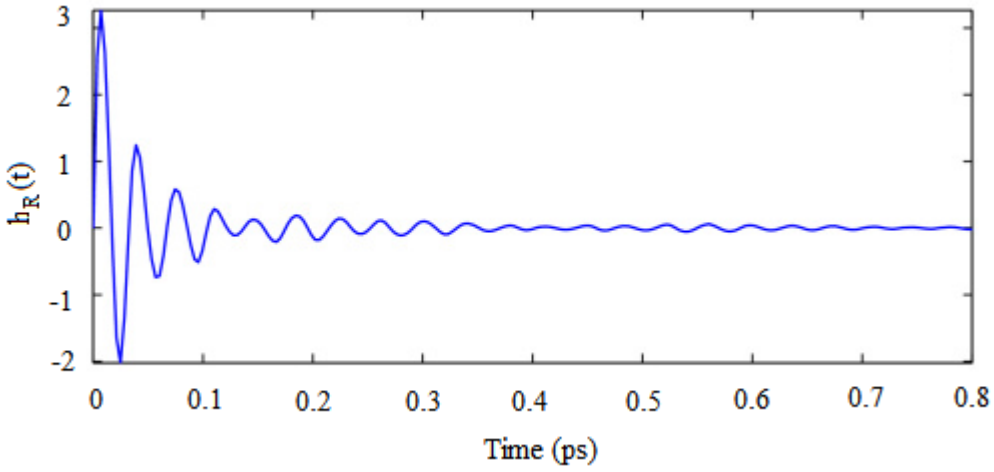

Fig 3.6: (b) Temporal form $h_R(t)$
(Courtesy: Nonlinear optics, GP Agrawal)

The supercontinuum generation for silica fibers at pump wavelength of 1550 nm is shown in Fig 3.7 for a fiber length of 2 m.

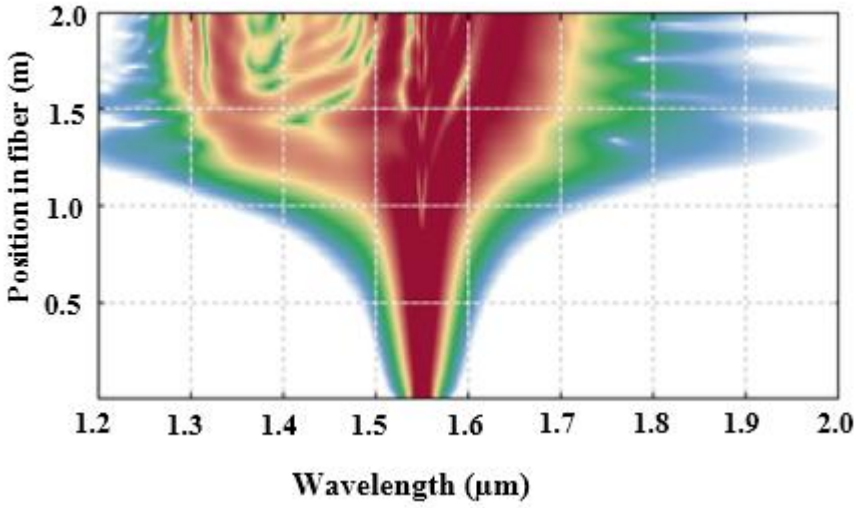

Fig 3.7. Super Continuum generation in a fiber
(Courtesy: RP Photonics)

The intensity of different wavelengths generated due to nonlinear process is different and can be equalized by using filter and amplifier. This will help in transmission at higher data rate since the messages can be modulated at different wavelengths with a single source.

Chapter 4

Optical simulation software and Numerical techniques

4.1 Introduction:

The field of optics has been constantly growing at a rapid rate. This growth is due to the advantages provided by the optical domain in terms of bandwidth, security etc. This growth is due to the extensive research work carried out by research scholars across the world. Research through experiment involves huge cost and is economically unviable. Hence to speed up the research and to reduce the cost, a number of optical simulation software based on various numerical technique have been developed. These software have accelerated the research work with minimal expense. The solution obtained through software simulation matches with the result obtained by experiments.

4.2 Optical simulation software:

Optical simulation software are used to design fibers, photonic devices, optics and opto-eletronic related systems to evaluate and optimise the design. The software solves the electromagnetic field by employing various numerical techniques like finite element method, finite difference time domain method, transfer matrix method, Variational method etc. The software are GUI based and doesn't require any formal knowledge of programming. Every software will have certain integrated module and is best suited for certain types of simulation.

4.2.1 Comsol Multiphysics:

Comsol Multiphysics is a finite element based simulation software for physics and engineering applications. The package is platform independent and has several module to simulate problems in different fields like MEMS, Chemical engineering, electromagnetics, mechanics etc. Comsol Multiphysics can be used to study the following

(a) Stationary and time-dependent (transient) studies.
(b) Linear and nonlinear studies.
(c) Eigen frequency, modal, and frequency response studies.

In optical domain the software can be used to design and simulate in following fields:

(a) Antennas+
(b) Waveguides and cavity resonators in microwave engineering
(c) Optical fibers
(d) Photonic waveguides
(e) Photonic crystals
(f) Active devices in photonics

The software can be used for electromagnetic field simulations and can handle time-harmonic, time dependent, Eigen frequency and Eigen mode problems in 2D/3D in all types of materials (both isotropic and anisotropic).

4.2.2 RP Fiber Power:

RP Fiber power software is developed by RP Photonics. It's a powerful modelling tool for designing and optimising fiber devices like fiber amplifiers, lasers, certain types of speciality fibers. It's a GUI based platform independent software. The features of RP fiber power are

(a) It can calculate various properties of all guided modes of weakly guiding fibers with radially symmetric refractive index profiles. The calculated properties include the transverse intensity distribution, the effective mode area, effective refractive index and group index and the group velocity distribution.

(b) It can model the behaviour of laser active ions with complicated and user-defined level schemes and it can include effects like spontaneous and stimulated emission, non-radiative transitions and energy transfer processes.

(c) It can handle an arbitrary number of pump and signal inputs and also deals with amplified spontaneous emission (ASE). The full radial dependence of doping profile and optical intensities are included.

The program RP Fiber Power was derived from JPLOT, from which the software inherited all general features like user interface, input commands, and calculation. In addition to JPLOT commands RP fiber has inbuilt function for the definition of fiber parameters, pump, signal and ASE. They also have inbuilt function for retrieving calculated results.

The software contains a mode solver, which can calculate the properties of all guided modes of the fiber, based on a given refractive index profile. The index profile needs to be real and

radially symmetric, but arbitrary radial dependence can be given. The mode solver solves using traditional radial method.

4.2.3 Optiwave:

Optiwave is one of the most versatile software available for simulation and analysis of optical and opto-electronics circuits. It is based on finite difference time domain and has different packages depending on type of design and simulation. Optiwave is extensively used in the design of DWDM communication elements design. It is based on the Beam Propagation Method (BPM) of simulating light passage through any waveguide medium. It has CAD environment and user is not required to have an indepth programming knowledge. OptiBPM is used for design and analysis of specific system like PCF, optical fibers and waveguides, communication system components like multiplexers, demultiplexers, switches couplers etc., OptiBPM allows designers to observe computer-simulated light field distribution and examine the radiation and the guided field, simultaneously. It's based on beam propagation method. For analysis of opto-electronic circuits or in an optical and electronic environment OptiSPICE software can be used. It supports the design, simulation and analysis of opto-electronic circuit at transistor level. OptiSPICE produces self-consistent solutions of opto-electro9nic circuits that contain feedback spanning both optical and electrical parts.

4.2.4 Lumerical Software:

The software is developed by Lumerical ltd. It is a software based on finite difference time domain method. It has various packages for optical simulation, electrical simulation, thermal solution and circuit simulation. Lumerical's component design product use multi-physics style simulations, workflows to model optical, electrical and thermal effects at the physical level. Lumerical's system design products simulate and optimise the performance of photonic integrated circuits. The optical simulation is carried out using FDTD method and key applications include metamaterials, photonic crystals, liquid crystal, integrated optics, OLEDs etc. The mode solution package provide environment to carry out modal analysis of fiber, waveguides and PCF by solving Maxwell's equations. It can build 1D, 2D and 3D models. It is compatible with dispersive and high index contrast materials. We can carry out bend loss, confinement low and modal area analysis for long lengths of fiber

4.3 Numerical techniques for electromagnetics:

Any system or model can be described in terms of equations with its parameters in the form of variable. These equations may be simple or complex. The equation can be solved either by analytical or numerical method. Analytical methods help in understanding the mechanism and physical effects through the model problem. To solve the equation through analytical method, high degree of expertise is required and is time consuming. For certain equations analytical solution is impossible and these methods are not suited to solve highly nonlinear equations. Numerical methods are often used to solve the differential equations with the help of computers. These methods are faster and provides solutions with acceptable level of accuracy. These methods are applicable to all types of systems and equations and are solved with the method of iteration [48]. There are various numerical techniques developed to solve equations.

4.3.1 Finite difference time domain:

It was developed by A Thom in 1920. The method was developed to solve the equations associated with hydrodynamic field. In this method the differential equation is reduced to a difference equation. The difference equation is then solved in the algebraic form. In this method, the value of dependent variable at the point in the solution region and the neighbouring points are related. The method can be applied for 1D, 2D and 3D models. The method involves three basic steps

(a) Dividing the solution region into a grid of nodes, finer the grid better is the accuracy but requires more computational resources.

(b) Approximate the given differential equation by finite difference equivalent that relates the dependent variable at a point in the solution region to its values in neighbouring points.

(c) Solving the difference equations subject to the prescribed boundary condition

The method has faster convergence and higher accuracy for objects with regular geometrical shapes.

4.3.2 Method of Moments:

It's a method to solve differential or an integral equation or combination of integro-differential equation. In this method moments are derived by multiplying with appropriate weighing function and then carry out integration. The method can be applied to variety of electromagnetic problems of practical interest. The problem analysis through method of moments involve following steps

(a) Derivation of appropriate integral equation.

(b) Conversion of the integral equation into a matrix equation using basis function and weighing function.

(c) Evaluation of matrix elements.

(d) Solving the matrix equation and obtaining permanent parameters of interest.

4.3.3 Transfer-matrix method (TMM):

It's a method used in acoustics and optical domain to analyse the propagation of the optical field or acoustic waves through a layered medium. The method is based on the fact that according to Maxwell's equation there are simple continuity conditions for the electric field across boundaries from one medium to the other. If field is known in the beginning the field at the end layer can be predicted from a simple matrix operation. The stack of layers can be represented as a system matrix, which is the product of individual layer matrices. Finally the system matrix may be converted in to reflection and transmission coefficients.

4.3.4 Variational Methods:

The methods that allow us to reduce the problem of integrating a differential equation to the equivalent Variational problem are usually called Variational methods. This method forms a common base for for method of moments and finite element method. The main advantage of Variational method is that it gives an accurate result without making excessive demands on computer storage and time. The Variational method of a given PDE is solved using two steps

(i) Apply a small perturbation in the given system equation

(ii) Determining the approximate solution using either sub domain, Galerikin or least square methods.

4.3.5 Finite element method:

Finite Element Method (FEM) is a numerical method that can be used to solve equations and models in the field of mechanics, heat flow, hydrodynamics, structural analysis, electromagnetic etc [49]. It's a very versatile tool for solving problems involving complex shapes. The analysis involves four steps.

(a) Discretizing the solution region into a finite number of sub regions or elements.
(b) Deriving governing equations for a typical element.
(c) Assembling of all elements in the solution region.
(d) Solving the system of equations obtained.

The discretisation involves dividing the region of solution into sub regions or subdomains which are called finite elements. The typical elements are a three node triangle, four node quadrilateral, five node rectangle and six node triangle. The three dimensional finite element include four node tetrahedron and eight node hexahedron. Finer the elements or mesh more is the accuracy and higher computational resources are required. After the elements are formed, individual element matrix are formed. After individual element co-efficient matrices are obtained, a global coefficient matrix is formed which will be an n x n matrix where n is the number of nodes of the structure. The global matrix will be combination of elements of individual element co-efficient matrices. The matrix can be used to solve the potential distribution of electric field or any other parameter in a structure.

Chapter 5

Supercontinuum Generation in co-axial multi-core silica fiber: Design and Analysis[1]

5.1 Introduction:

Silica or silicon dioxide is a chemical compound that is an oxide of silicon with chemical formula SiO_2. Silica is most commonly found in nature as quartz and sand. Silica is one of the most complex and most abundant families of materials existing both as several minerals and being produced synthetically. Some of the products are fused quartz, crystal, fumed silica, silica gel and aero gels. Applications range from structural materials to microelectronics.

Initial fiber manufacture was carried out using silica because of the transparency of the material. Till date the telecommunication fibers are manufactured using silica as dominant material. For core doping is carried out using GeO_2.

5.2 Losses in Silica Fiber:

Electromagnetic waves of wavelength between ultra violet region and infra-red region experiences different attenuation due to material absorption [1]. Figure 5.1 shows a possible optical attenuation against wavelength characteristic for pure glass. It may be observed that there is a fundamental absorption edge, the peaks of which are centred around the UV region. This is due to stimulation of electron transitions within the glass by higher energy excitations. The tail of this peak may extend into the window region of shorter wavelengths. In the IR region and far IR region normally wavelengths above 7 μm, fundamentals of absorption band from the interactions of photons with molecular vibrations within the glass occur. These give absorption peaks which again extend into the window region. The strong absorption band occur due to oscillations of structural units within the glass. The attenuation is least around 1.5 μm. Silica has a relatively low nonlinear refractive index of $2.7 * 10^{-16}$ cm^2/W for wavelengths around 1.5 μm. The low nonlinear refractive index indicates that the nonlinear effects are less compared to a material with higher nonlinear refractive index with

[1] The result of this chapter has been communicated to Optik-International journal for Light and Electron Optics

same input power. Due to this reason silica base optical fiber are less preferred for nonlinear applications.

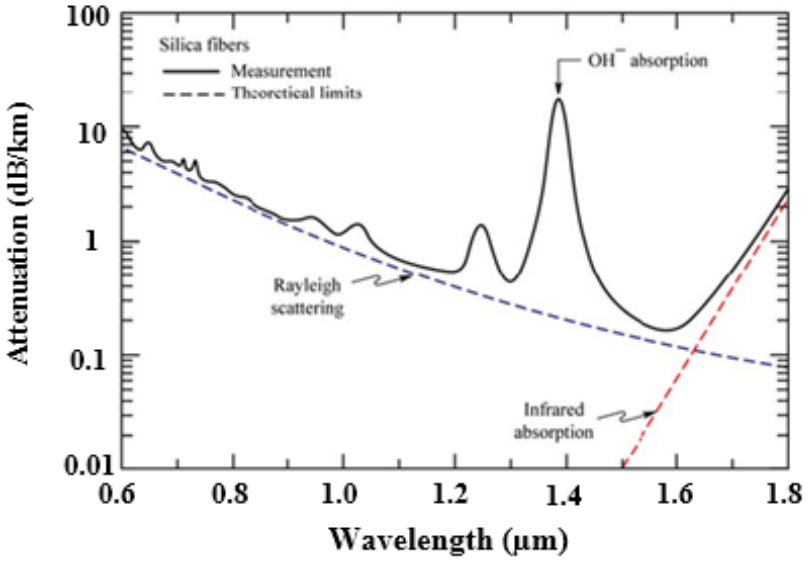

.Fig 5.1 Attenuation characteristics against wavelength (silica)
(Courtesy: Optical Fiber Communication; John M Senior)

SCG at visible region in a silica fiber will experience losses due to intrinsic material absorption. Also the SCG will not be efficient due to its low nonlinear refractive index. The window between 400 nm to 800 nm will experience attenuation as evident from Fig 5.1

5.3 Fiber Design:

To achieve a wider flat continuum, an all normal dispersion fiber, with zero dispersion at pump wavelength is a prerequisite. Using Sellmeier's equation [50], refractive index of silica has been calculated and has been taken as 1.563.

$$n(\lambda) = \sqrt{(1 + \frac{b_1\lambda^2}{\lambda^2 - c_1^2} + \frac{b_2\lambda^2}{\lambda^2 - c_2^2} + \frac{b_3\lambda^2}{\lambda^2 - c_3^2})} \qquad (5.1)$$

where, b_1, b_2, b_3, c_1, c_2 and c_3 are coefficients. The value of coefficients are b_1 = 0.6961663, b_2 = 0.4079246, b_3 =0.8974794, c_1 = 0.0684043, c_2 = 0.1162414 and c_3 = 9.896161

The core is kept at a higher refractive index with co-axial multi-core design and with step index refractive index profile. The radius of the core is 4 μm. The entire core is divided in steps of 0.8 μm and has a refractive index profile as shown in Fig 5.2.

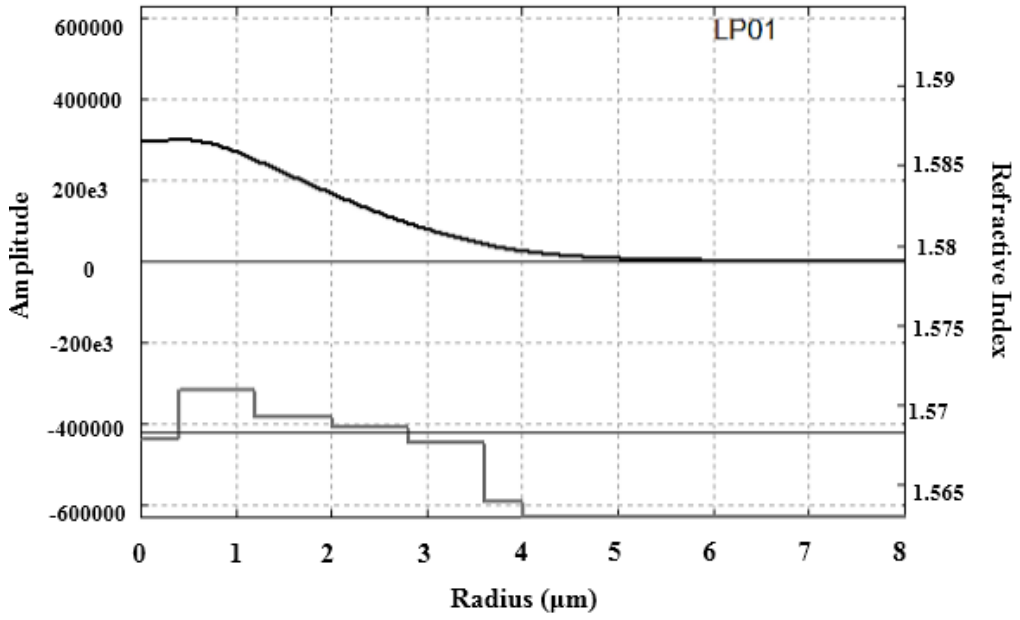

Fig 5.2 Refractive index profile of silica fiber

In the above design the fiber is multimode. Four modes are propagating through the fiber which has been shown in Fig 5.3. The number of modes are solved by solving Maxwell equation using radial method [51]. At shorter wavelength, the core radius should be very small to achieve single mode. At these wavelengths dispersion will be higher. Designs to achieve single mode were yielding very high dispersion at pump wavelength and also at region of interest. Hence the design was frozen at 4 µm.

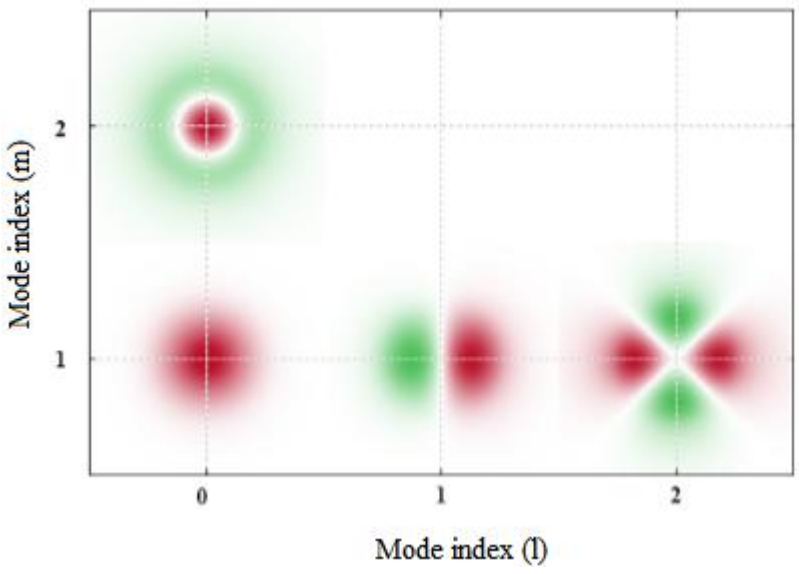

Fig 5.3. Modes in silica fiber

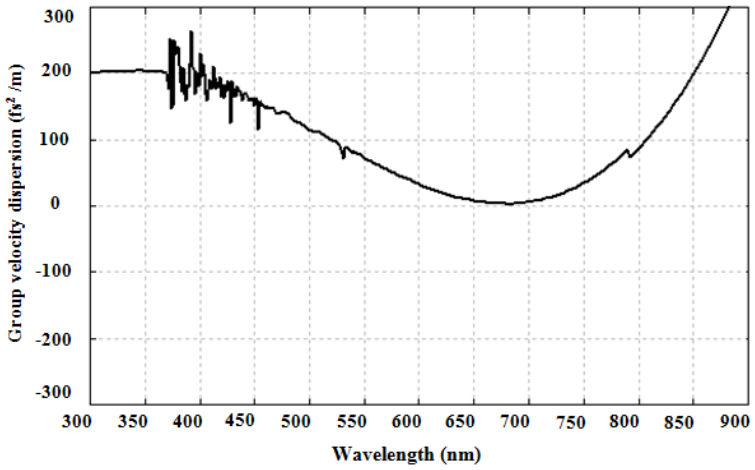

Fig. 5.4 Chromatic dispersion profile of designed silica fiber

The dispersion profile in Fig 5.4 indicates that fiber has all normal dispersion profile ($\beta_2>0$). The dispersion in the visible region that is between 400 nm to 800 nm is less than 200 fs^2/m. Due to the above dispersion profile there will be losses due to dispersion between 400 nm to 650 nm and again between 700 to 800 nm. These losses can minimized by using higher energy pulse as discussed previously. Losses beyond 900 nm due to dispersion will be very high due to the design.

Secant hyperbolic pulse has been used in the simulation. It is governed by the equation [14]

.o (5.2)

where, $t_0 = T_{FWHM} / 1.7627$ and P_0 is Peak power and C is the chirp coefficient. The secant hyperbolic pulse is depicted in Fig 5.5

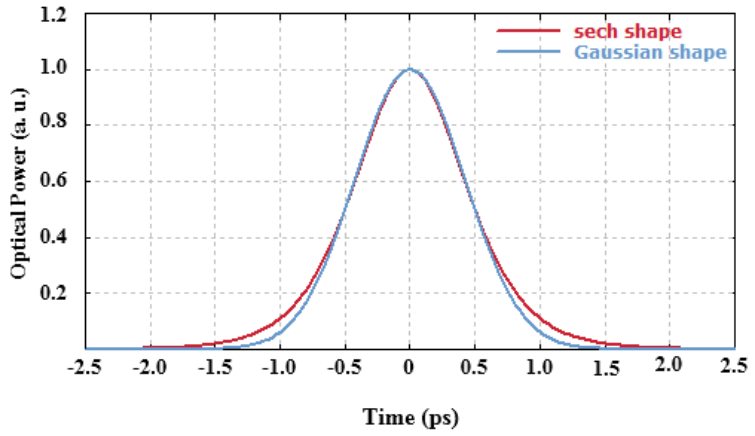

Fig 5.5 Secant hyperbolic pulse and Gaussian pulse

5.4 Results and discussion:

SCG has been studied by varying pulse width, fiber length and pulse energy. The effect of these parameters on spectrum width has been plotted.

5.4.1 Effect of pulse width and length on power output and spectrum width:

The various pulse widths used are 500 fs, 400 fs, 300 fs, 200 fs and 100 fs, with a pulse energy of 1 nJ. Effect of fiber length and pulse width on power output and spectrum broadening has been shown in Fig 5.6 and Fig 5.7 respectively. The results has been plotted for various fiber lengths till 4.5 m.

At shorter pulse width (100 fs) the rate of change of intensity is rapid which results in an effective self-phase modulation as described in chapter 2. As the pulse width increases the rate of change of intensity decreases. This results in decreasing self-phase modulation.

As the pulse propagates along the fiber, the pulse is subjected to various nonlinear effects. The pulse undergoes self-phase modulation, cross-phase modulation, four wave mixing and stimulated Raman scattering. As the pulse propagates along the fiber these nonlinear effects result in broadening of the fiber. At an optimum length, all the nonlinear effects are complete resulting in maximum spectral broadening as show in Fig 5.7. Beyond this length spectral broadening is negligible. Due to the nonlinear effect during the propagation the average power of the spectrum increases. The spectrum will have maximum power when all the nonlinear effects are complete. Beyond this length the spectrum experiences attenuation resulting in lower power output as shown in Fig 5.6.

Figure 5.8 shows the variation of average power of the spectrum and spectrum width against fiber length for a pulse width of 100 fs with pulse energy 1 nJ. Figure 5.9 and Fig 5.10 shows continuum for pulse width of 100 fs and 200 fs at z=1.5 m (fiber length), pulse energy 1 nJ. The pulse power for 100 fs is 9.5 kW and for 200 fs is 3.7 kW. The power of the continuum can be calculated using the pulse power.

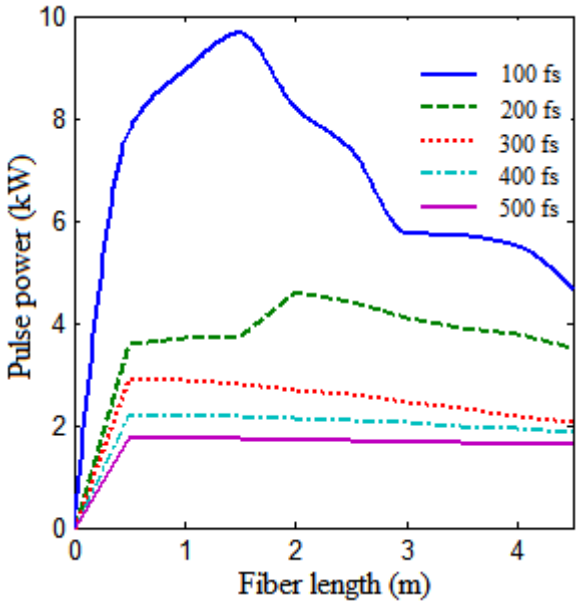

Fig.5.6 Pulse power output vs Fiber length for different pulse width

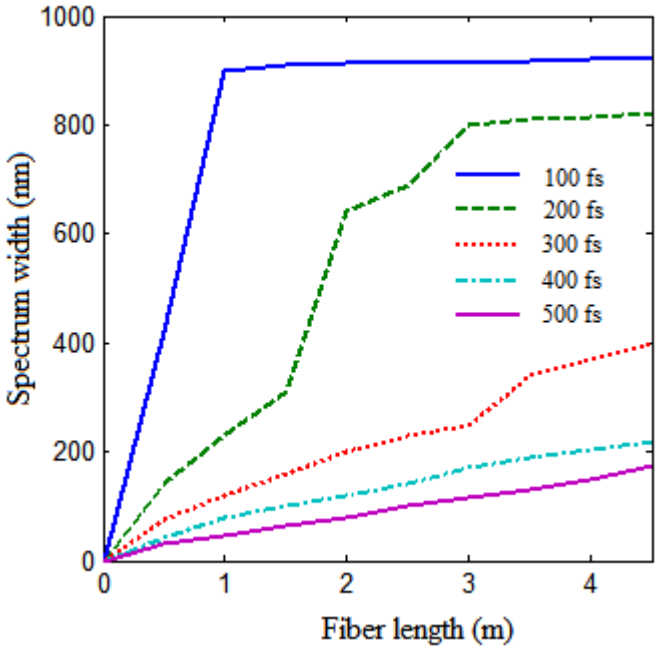

Fig. 5.7 Spectrum width vs fiber length for different pulse width

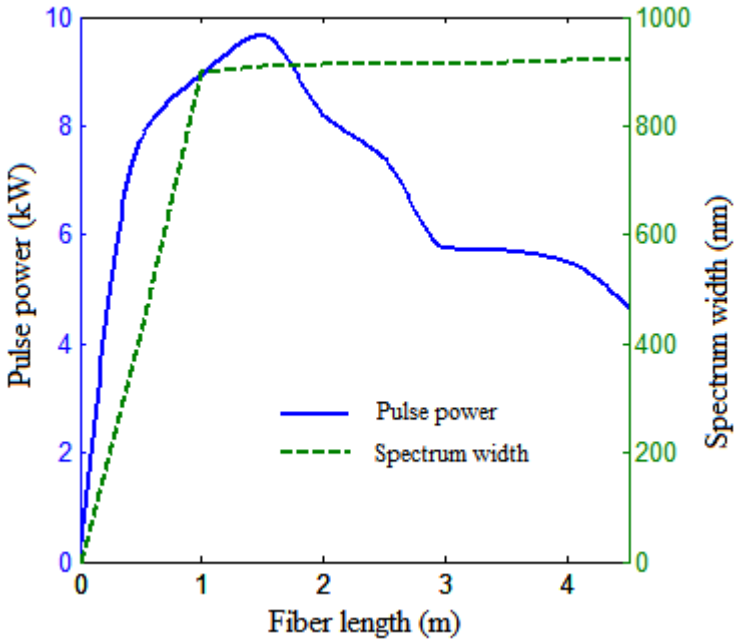

Fig. 5.8 Pulse power and spectral width against fiber length

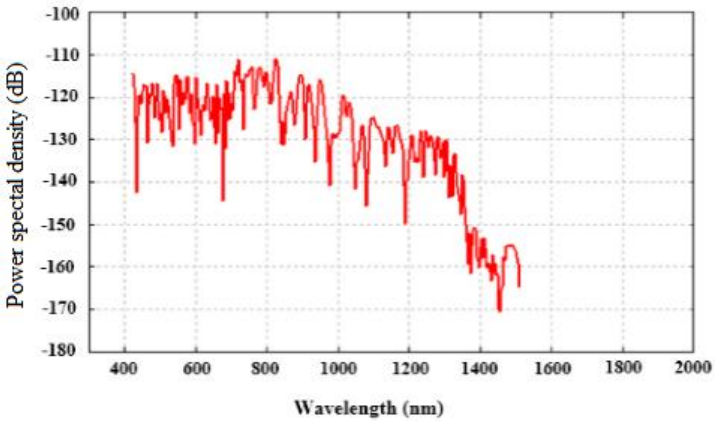

Fig. 5.9 Continuum at z= 1.5 m, pulse width of 100 fs pulse energy = 1nJ, Pulse Power =9.5 kw,

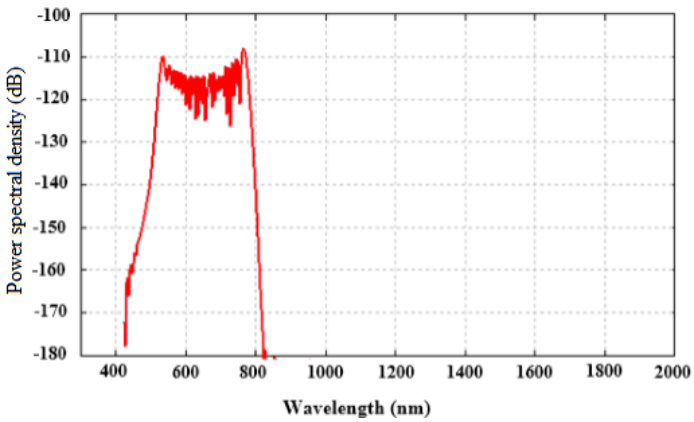

Fig 5.10 Continuum at z=1.5m pulse width of 200 fs pulse energy= 1nJ Pulse power =3.7 kW

5.4.2 Effect of pump power energy:

The spectral width of the continuum varies with pump power. Intensity is the ratio of power to the core area. As the pump power is increased the intensity increases since the area of the core is constant. This results in higher nonlinear effects leading to a broader continuum. Figure 5.11 shows the variation of spectrum width with respect to pulse energy. It can be seen that, if the pulse width is kept constant and pulse energy is increased the spectrum width will increase.

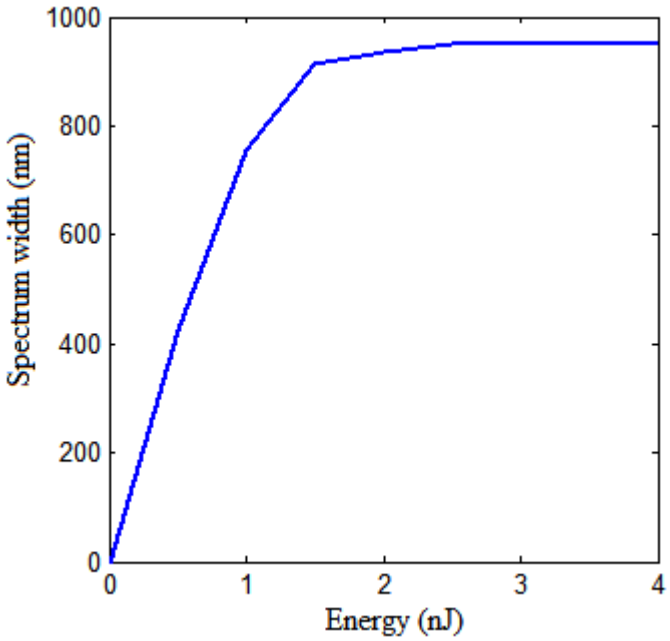

Fig 5.11. Spectrum width at 100 fs for different pulse energy

The increase in energy will not result in the increase in spectrum but will be constant after the maximum spectrum width is achieved. However when pulse energy is increased with pulse width kept constant the spectrum flatness improves. This is because the energy will compensate for the material and dispersion losses which occur at extremely longer wavelength and shorter wavelengths. Figure 5.12 (a) and Fig.5.12 (b) represents continuum at two different pulse energy of 1 nJ and 2.5 nJ with all other parameters kept constant.

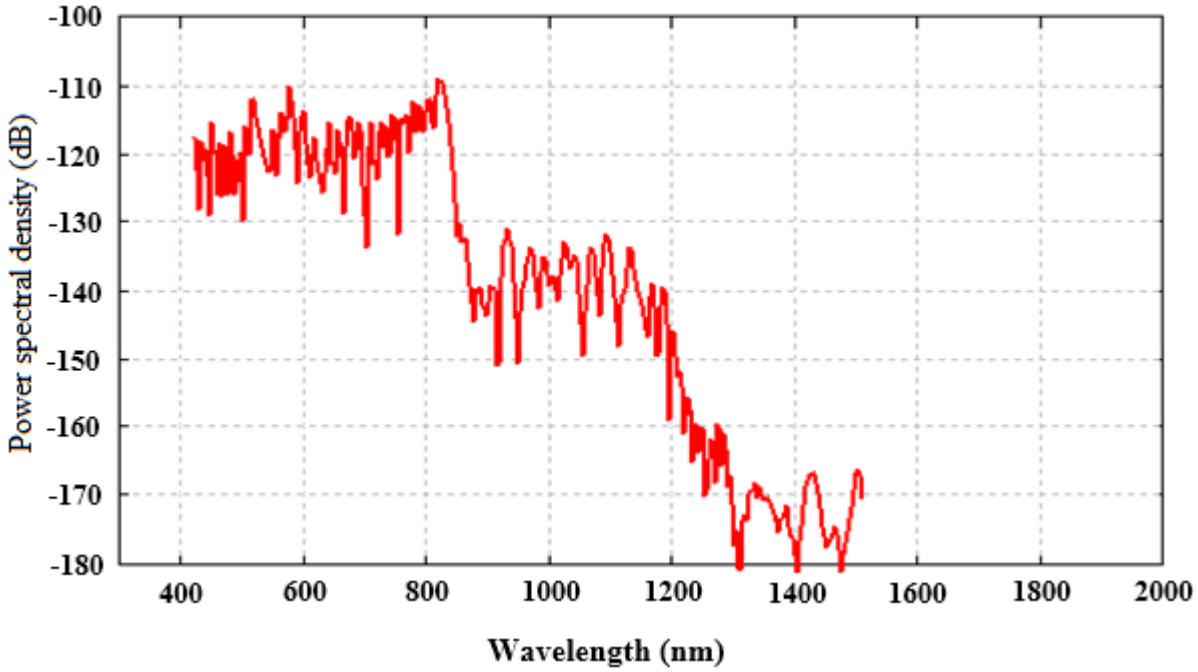

Fig 5.12 (a) Spectrum at 1nJ at a fiber length 2m pulse width 100 fs

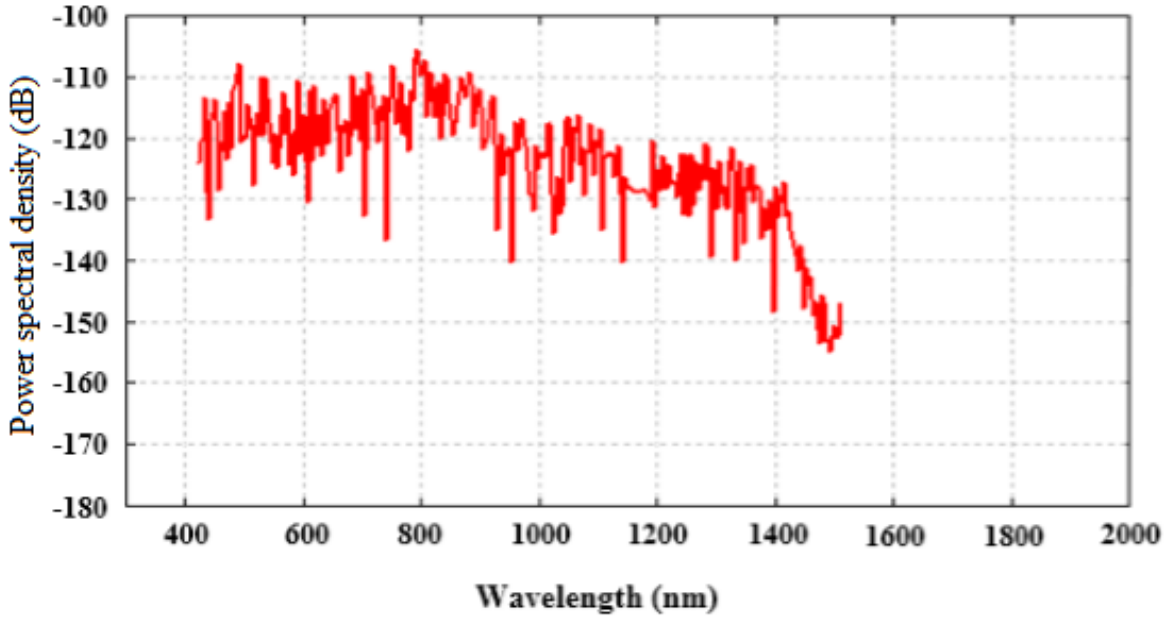

Fig 5.12 (b) Spectrum at 2.5 nJ at fiber length 2m pulse width 100 fs

It is evident that at higher pulse energy continuum is more flat compared to continuum obtained at lower pulse energy. The drop in optical power in Fig 5.12 (b) is gradual as compared to the drop in optical power in Fig 5.12 (a) at 800 nm wavelength.

5.5 Conclusion:

In this project the simulation of the SC in a co-axial multi core silica fiber has been carried out at 660 nm to generate a continuum at visible region. Various geometrical parameters which affect the continuum are studied by employing commercially available RP fiber power software. The simulation involved a design of fiber to achieve zero dispersion at pump wavelength. During the design of the proposed fiber structure, various parameters (like core radius, refractive index core and also the number of cores) have been varied to achieve all normal dispersion, flat dispersion and also zero dispersion at the pump wavelength. The proposed optimized design of the fiber is very useful for SCG. The variation in parameters of fiber and pulse, affect the spectrum broadening. A flat spectrum has been obtained using a 100 fs pulse, with a pulse energy of 2.5 nJ with a fiber length of 2m as shown in Fig 5.13.

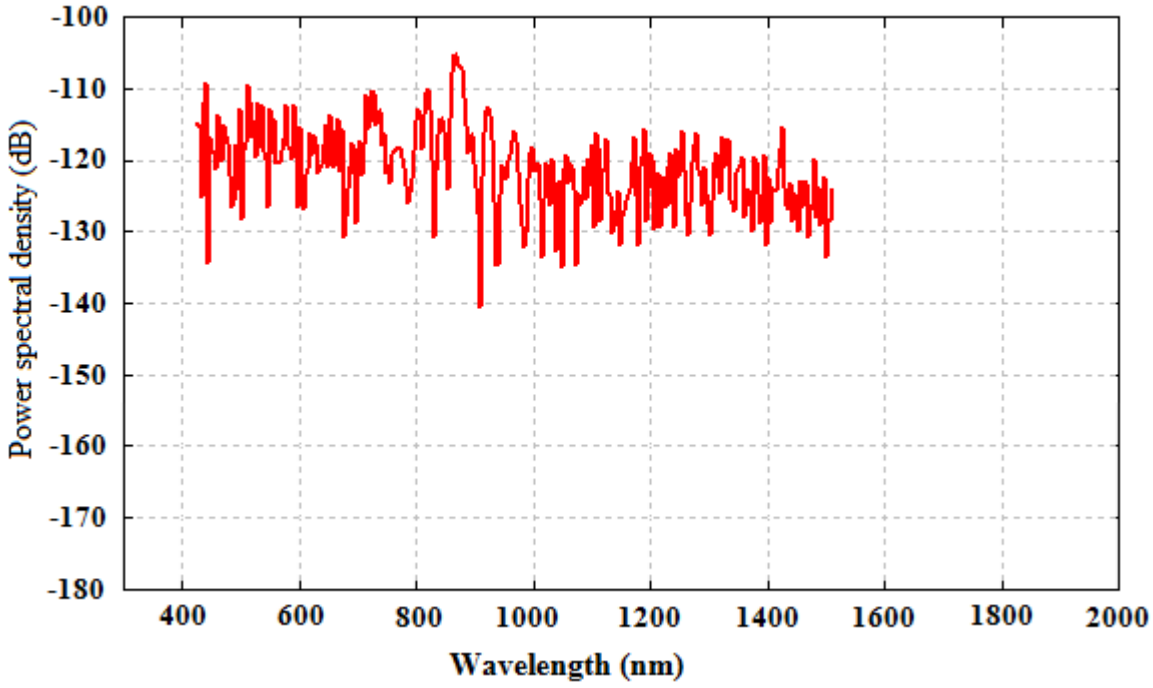

Fig 5.13. Spectrum at fiber length 2 m, pulse width 100 fs, pulse energy 2.5 nJ

Chapter 6

Supercontinuum Generation in co-axial multi-core Tellurite fiber: Design and Analysis

6.1 Introduction:

Silica fibers have been extensively used in telecommunication and medical field. Its application in nonlinear system is limited due to its low nonlinear refractive index. The SCG in a silica fiber will experience more losses and more power, and longer length of fiber is needed to obtain a sufficiently large spectrum compared to a material with higher nonlinear refractive index.

Tellurite or TeO_2 is another material from which fibers have been drawn and has good thermal stability, viscosity and durability along with high nonlinear refractive index. The table below compares various parameters of Silica based and Tellurite based fibers.

Table 6.1. Comparison of various parameters of silica and tellurite as host materials for super continuum generation. [52]

Material Properties	**Silica (SiO_2 based)**	**Tellurite (TeO_2 based)**
Refractive index n at 0.66 μm	1.53	2.093
Nonlinear refractive index n_2 ($\times 10^{-20}$ m /W)	2.5	20–50
λ_0, zero dispersion wavelength of material (μm)	~1.3	~2
IR longwave transmission limit	up to 2.5 μm	6–7 μm
Thermal stability for fiber drawing	excellent	good
Viscosity around fiber drawing temperature	flat	steep
Durability in environment	excellent	good
Toxicity	safe	safe

6.2 Losses in Tellurite fibers:

The infrared cut-off wavelength of a glass is principally determined by the overtone of fundamental network vibrations which is referred to as multi-phonon absorption [53]. For low phonon energy glasses, the multi-phonon edge is shifted to longer wavelengths. Glass material like TeO_2 having low bond strength exhibit low phonon energies that is maximum energy of the network vibration within the glass is low compared to with that of other compound glasses like silica. Also the TeO_2 glasses will be subjected to other absorption along with multi-phonon absorption such as scattering, impurity absorption and OH or hydroxyl absorption as shown in Fig 6.1. These absorptions lead to the formation of broad and intense absorption bands in the mid-IR range owing to fundamental vibrations in this range [54]. Therefore water contents in the material must be minimised to achieve high mid-IR transparency which is possible in low phonon energy glasses. Tellurite glasses combine the attributes of low absorption between 0.35-5 µm with good glass stability, high rare earth ion solubility and corrosion resistance.

Tellurite has a higher nonlinear refractive index. The nonlinear refractive index of tellurite is about 29.2 x 10^{-20} m/W. This is almost ten times the silica fiber. Hence this material is best suited for nonlinear applications.

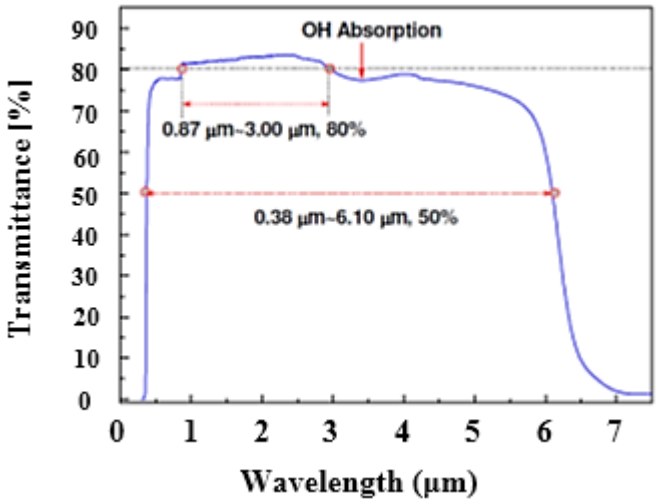

Fig 6.1 Losses in Tellurite Fiber

(Courtesy: Aoxiang Lin, Aidong Zhang, Elizabeth J. Bushong and Jean Toulouse 'Solid Core Tellurite Fiber for Infrared and nonlinear application'. OSA Vol 17, 19, 2009)

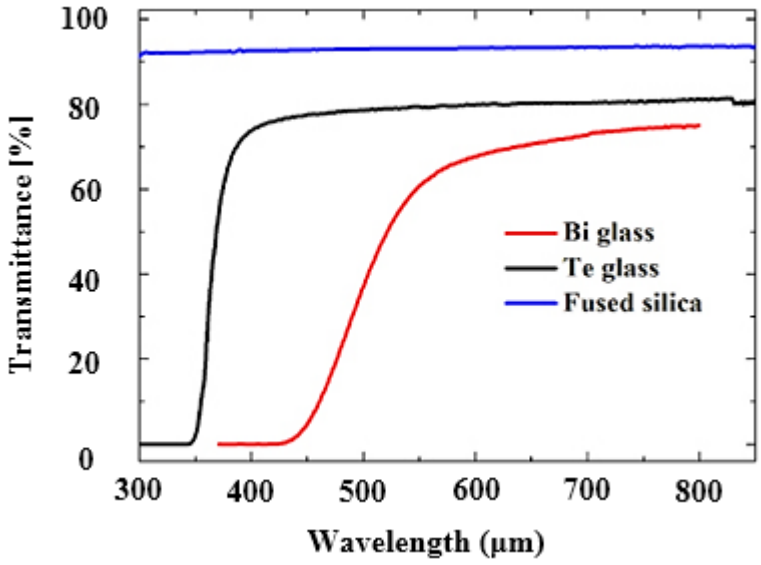

Fig 6.2 Transmittance property of various glasses

Figure 7.2 shows the transmittance characteristics of telluride. Telluride has a strong absorption up to 350 nm and a low loss folder between 400 nm to 4 μm. The ZDWL of tellurite glass is around 2 μm as compared to 1.3 μm of silica [52].

6.3. Fiber Design:

The inescapable features that are required for a fiber involved in SCG are zero or minimum dispersion at pump wavelength and a flat dispersion in the region of interest. Using Sellmeier's equation [55], refractive index of tellurite has been calculated and has been taken as 2.093.

$$n(\lambda) = \sqrt{(1 + \frac{b_1\lambda^2}{\lambda^2 - c_1^2} + \frac{b_2\lambda^2}{\lambda^2 - c_2^2} + \frac{b_3\lambda^2}{\lambda^2 - c_3^2})} \qquad (6.1)$$

where, b_1, b_2, b_3, c_1, c_2 and c_3 are coefficients. The value of coefficients are $b_1 = 1.212$, $b_2 = 2.157$, $b_3 = 0.1891$, $c_1 = 0.06068$, $c_2 = 0.0007068$ and $c_3 = 45.19$.

The core is kept at a higher refractive index with co-axial multi-core design and with step index refractive index profile as shown in Fig 6.3. The radius of the core is 4 μm. The entire core is divided in steps of 0.8 μm.

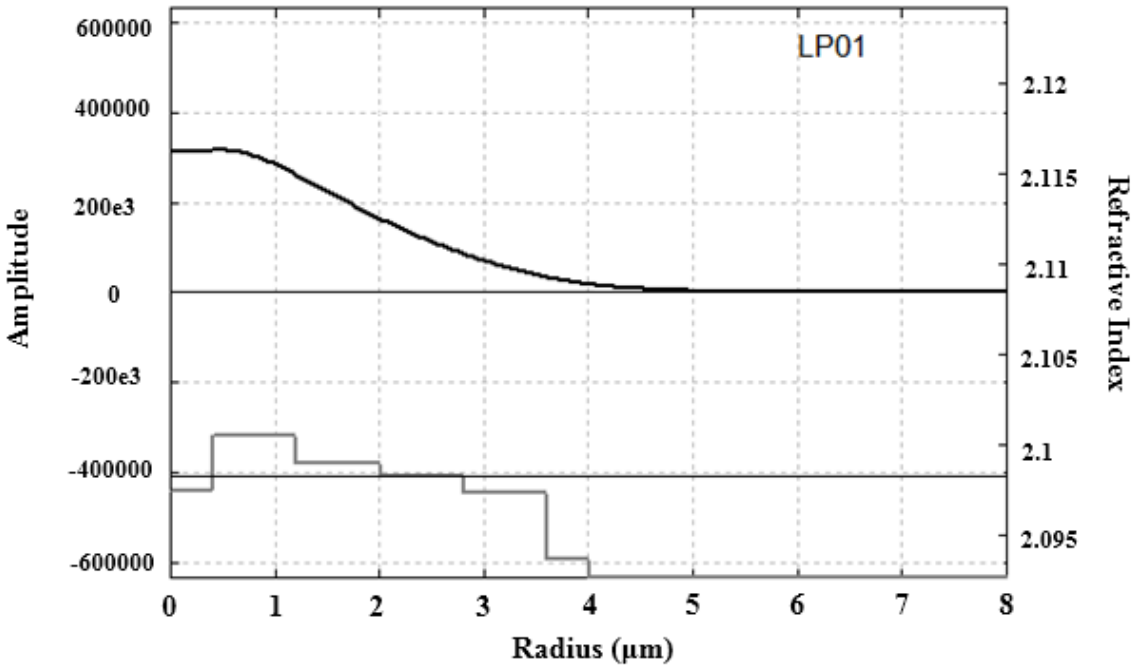

Fig 6.3 Refractive Index Profile of Tellurite Fiber

Five modes are propagating in the fiber designed with above specification. At smaller wavelength, the core radius is to be small to propagate single mode. Reducing the core radius increases the dispersion at pump wavelength. Figure 6.4 shows the modes propagating the fiber.

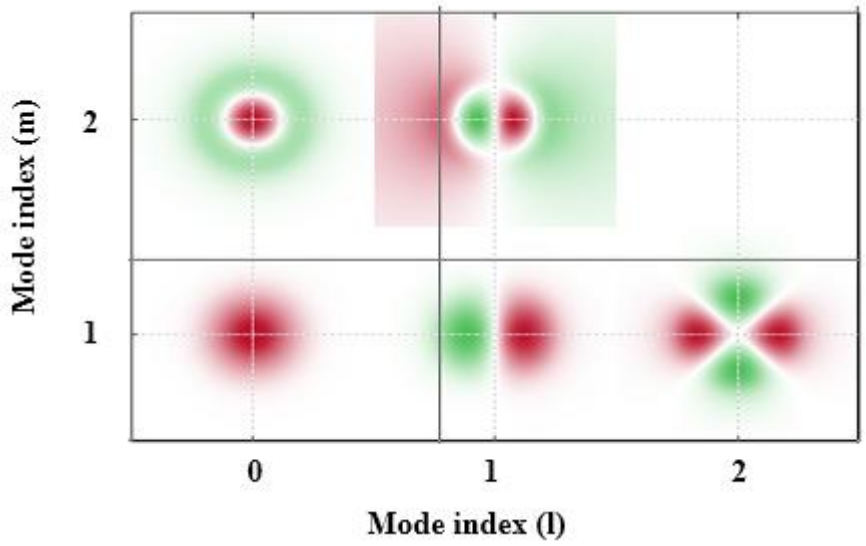

Fig 6.4 Fiber modes

The fiber is designed for having zero dispersion at pump wavelength as shown in Fig 6.5. This will ensure that the pulse that is launched into the fiber will not spread thus keeping the shape intact. This will help in efficient self-phase modulation and thus leading to a wider continuum.

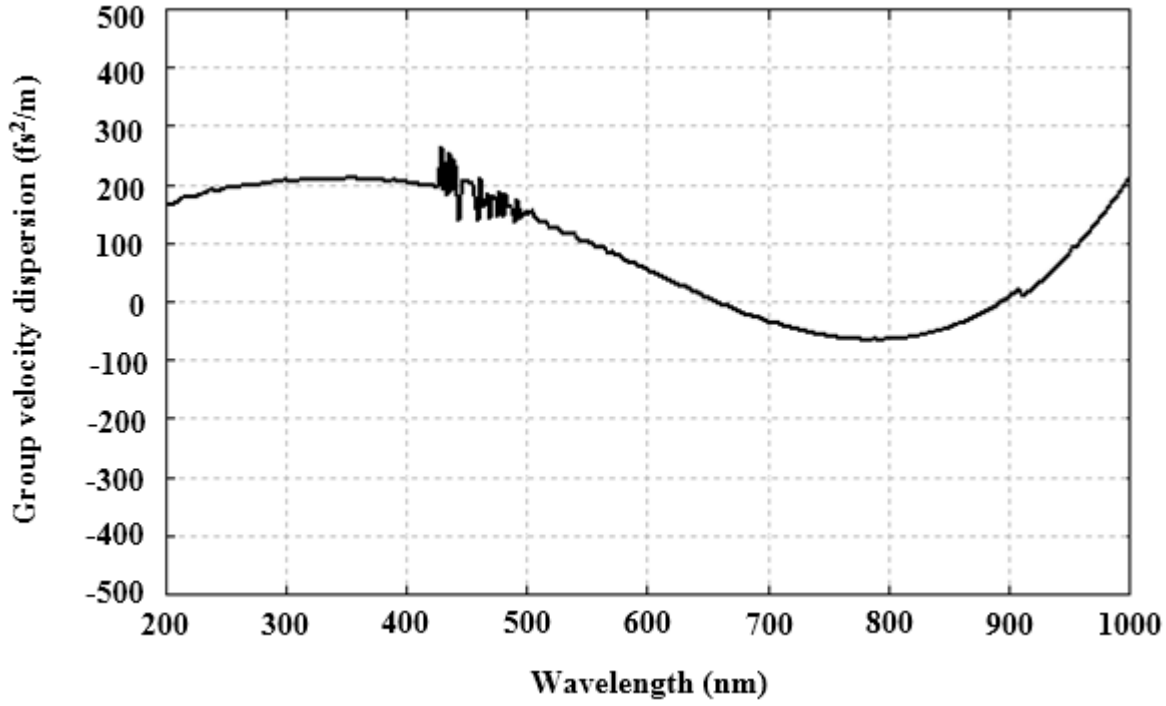

Fig 6.5 Dispersion profile of Tellurite Fiber

The dispersion profile indicates that fiber has anomalous dispersion region ($\beta_2<0$) and normal dispersion profile ($\beta_2>0$). The longer wavelength will have to propagate in the anomalous dispersion region. The dispersion in the visible region that is between 400 nm to 800 nm is between -100 to 200 fs^2/m. Ideally the dispersion should be flat to obtain a flat continuum. Due to the above dispersion profile there will be losses due to dispersion between 400 nm to 650 nm and again between 700 to 800 nm. These losses can minimized by using higher energy pulse. Losses beyond 900 nm due to dispersion will be very high due to the design.

Secant hyperbolic pulse is used for the simulation.

6.4 Results and discussion:

SCG has been studied by varying pulse width, fiber length and pulse energy. The effect of these parameters on spectrum width has been plotted.

6.4.1 Effect of pulse width and length on power output and spectrum width:

The various pulse widths used are 400 fs, 300 fs, 200 fs and 100 fs, with a pulse energy of 0.1 nJ. Effect of fiber length and pulse width on power output and spectrum broadening has been shown in Fig 6.6 and Fig 6.7.The results has been plotted for various fiber lengths till 4m. It can be seen that even with a pulse energy of 0.1 nJ, a broader spectrum can be obtained. This is due to higher nonlinear refractive index.

At shorter pulse width (100 fs) the rate of change of intensity is rapid which results in an effective self-phase modulation. As the pulse width increases the rate of change of intensity decreases. This results in decreasing self-phase modulation.

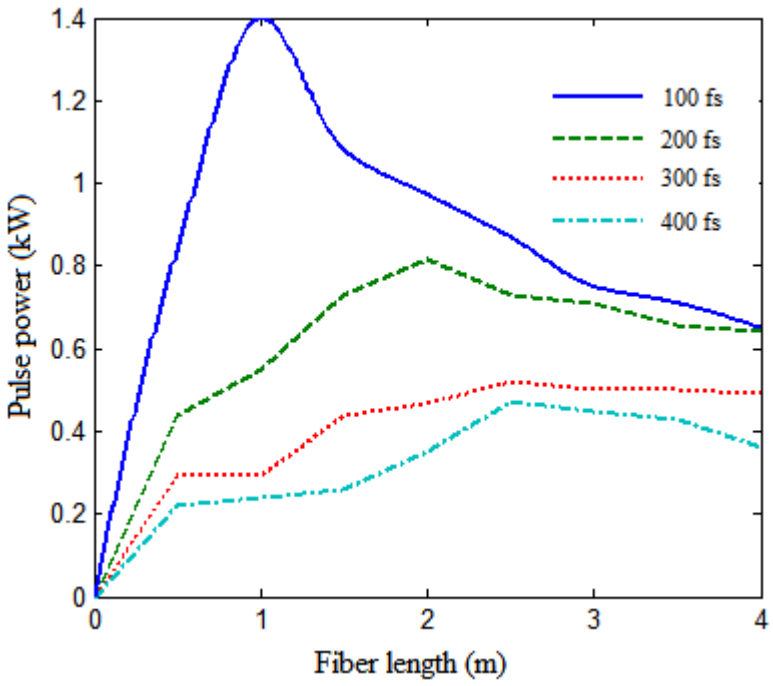

Fig 6.6 Pulse power for various pulse width at different fiber length

As the pulse propagates along the fiber, the pulse is subjected to various nonlinear effects. The pulse undergoes self-phase modulation, cross-phase modulation, four wave mixing and stimulated Raman scattering. As the pulse propagates along the fiber these nonlinear effects result in broadening of the fiber. At an optimum length, all the nonlinear effects are complete resulting in maximum spectral broadening as show in Fig 6.7.

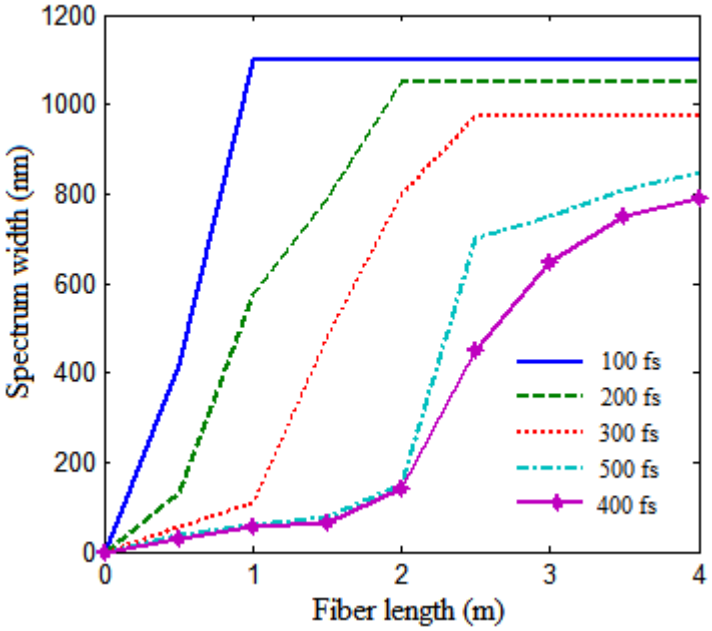

Fig 6.7 Spectrum broadening for different pulse width at different fiber length

Beyond this length spectral broadening is negligible. Due to the nonlinear effect during the propagation the average power of the spectrum increases. The spectrum will have maximum power when all the nonlinear effects are complete. Beyond this length the spectrum experiences attenuation resulting in lower power output as shown in Fig6.8.

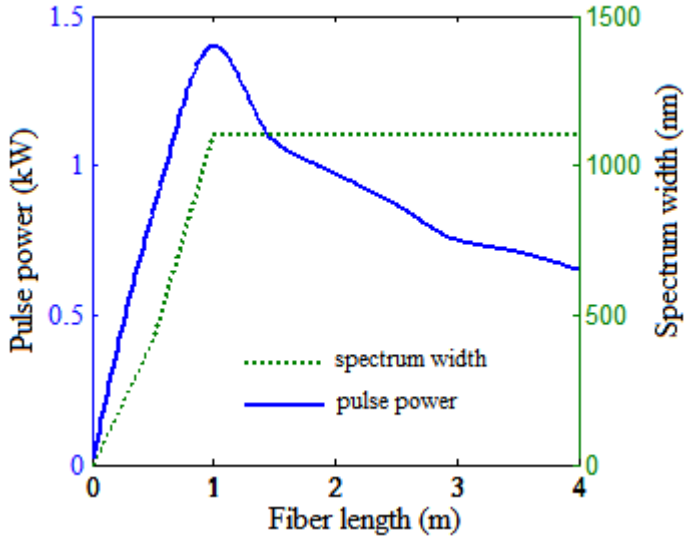

Fig 6.8 Comparison of spectral broadening and pulse power at different fiber length

Figure 6.8 shows the variation of average power of the spectrum and spectrum width against fiber length for a pulse width of 100 fs with pulse energy 0.1 nJ. Figure 6.9 (a) and Fig 6.9 (b) shows continuum at for pulse width of 100 fs and 200 fs at z=1 m (fiber length), pulse

energy 0.1 nJ. As the pulse width increases, the broadening of spectrum is limited and also losses are high at extremely longer and shorter wavelengths.

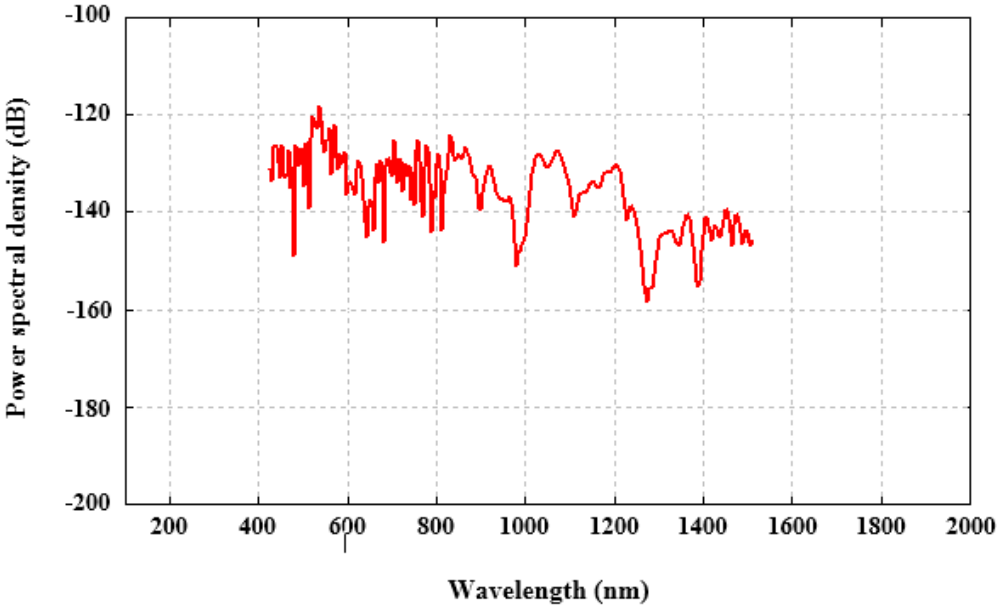

Fig 6.9 (a) Spectrum for 100 fs pulse width at fiber length of 1m

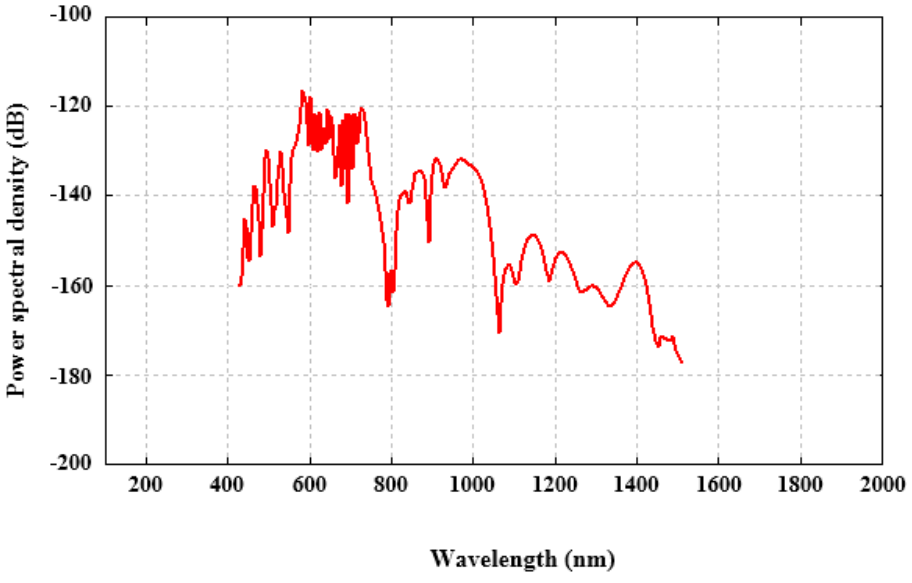

Fig 6.9 (b) Spectrum for 200 fs pulse width at fiber length of 1m

6.4.2 **Pulse Energy vs Spectrum**

If the pulse width is kept constant and pulse energy is increased the spectrum width will increase. The increase in energy will not result in the increase in spectrum but will be constant after the maximum spectrum width is achieved. However when pulse energy is increased with pulse width kept constant the spectrum flatness improves. This is because the energy will compensate for the material and dispersion losses which occur at extremely longer wavelength and shorter wavelengths.

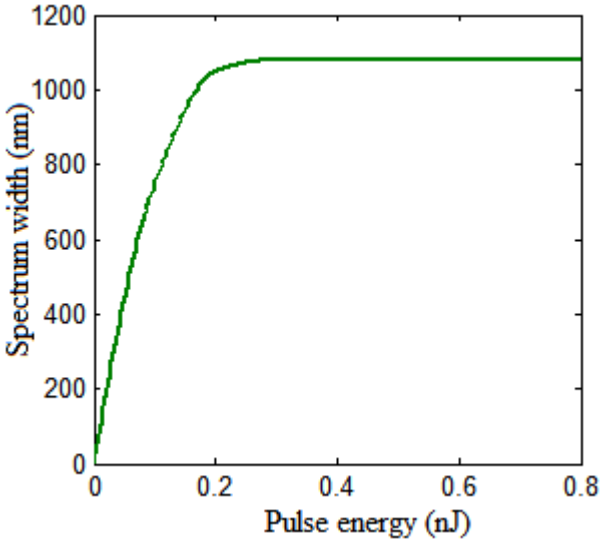

Fig 6.10 Spectrum broadening for different pulse energy at constant fiber length

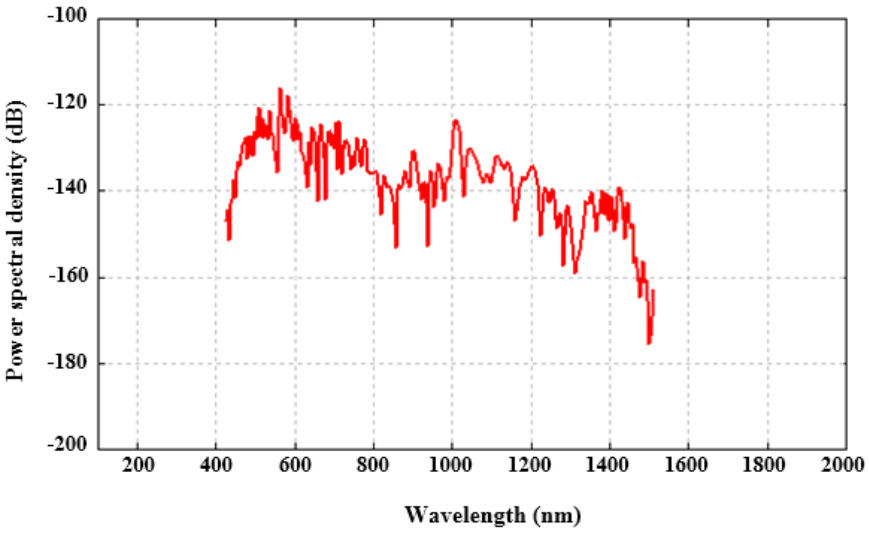

Fig 6.11 (a) Spectrum for pulse energy 0.1 nJ

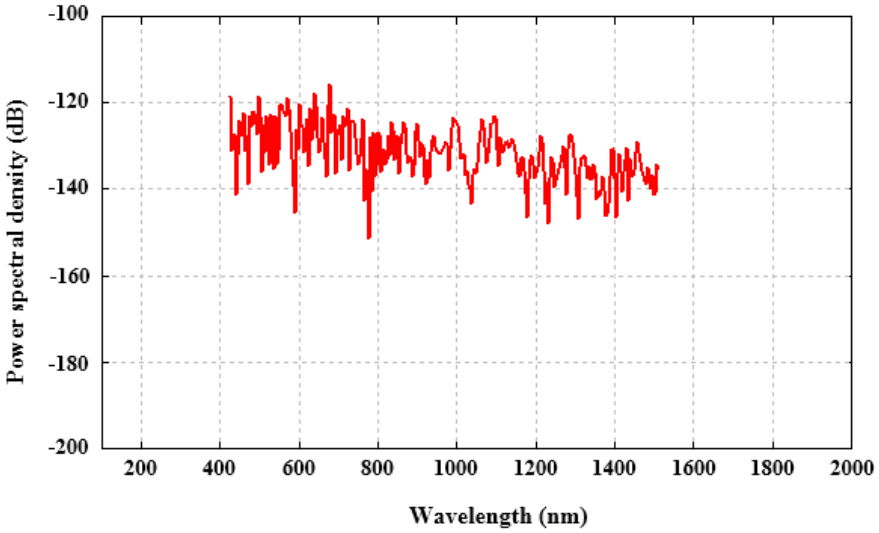

Fig 6.11 (b) Spectrum for pulse energy 0.2 nJ

Figure 6.11(a) and Fig 6.11(b) represents plot of power spectral density against wavelength at energy levels of 0.1 nJ and 0.2 nJ respectively. The spectrum at 0.1 nJ experiences a loss as the wavelength increases as in Fig 6.11(a). The spectrum at 0.2 nJ energy has a flat spectrum and losses due to material and dispersion is compensated due to the additional pulse energy.

6.5. Conclusion

In this project, the simulation of the super continuum in a co-axial multi core tellurite fiber has been carried out at 660 nm pump wavelength to generate a continuum in visible region. Various geometrical parameters which affect the continuum are studied by employing commercially available RP fiber software. The tellurite fiber has a sharp cut-off at 400 nm in the UV region. In the far IR region the fiber shows better transmittance properties compared to silica.

The nonlinear coefficient of tellurite is high compared to silica. This feature attracts tellurite fiber for nonlinear applications like SCG. The simulations were carried out by varying geometrical parameters like core radius and cladding radius to achieve zero dispersion at pump wavelength and all normal dispersion. The design was also optimized by varying refractive index of core and a co-axial multicore step index fiber was designed.

Simulations were carried out to study the effect of various pulse and geometrical parameters like pulse width, length of the fiber and energy of the pulse. The continuum was observed

and analyzed for changes in all the above parameters. It was observed that the process of SC requires adequate length of fiber for interaction of fields. At an optimum length the pulse power is maximum, with maximum broadening. Beyond this length the spectrum experiences losses as it propagates along the fiber.

.

Chapter 7

Ultra Broadband mid-IR Supercontinuum Generation in $Ge_{11.5}As_{24}Se_{64.5}$ based Chalcogenide Graded-Index Photonic Crystal Fiber: Design and Analysis[2]

7.1 Introduction:

Supercontinuum generation (SCG) is the phenomenon of broadening of ultra-short high intensity laser pulse when it propagates through a nonlinear medium of adequate length with very small effective area. The phenomenon is due to various nonlinear effects as discussed in chapter 2. The study on SCG has gained importance since the spectrum generated due to this process has high spatial coherence and has found useful in many applications in field of frequency metrology, optical coherence tomography, molecular spectroscopy, biomedical imaging, gas sensing, food quality control and early cancer detection [56-63].

The mid-IR region is important because the fundamental molecular vibration absorption bands are stronger compared to the overtones and combination absorption bands is situated in the near-IR region. The composition of molecular structure of the substance can thoroughly be understood with the help of Mid-IR spectroscopy and also carry out non-intrusive diagnostics [64].

SCG has been carried out in silica as well as nonsilica glasses. Nonsilica glasses include ZBLAN (ZrF_4- BaF_2-LaF_3-AlF_3-NaF), Tellurite, Bismuth and Chalcogenide glasses. Since the inception of optic fibers silica has been the standard material for fiber manufacture and the manufacturing process has been perfected over years of research. Commercially silica based step index, graded index and photonic crystal fibers are available for telecommunication and certain nonlinear applications from deep ultraviolet to near IR region. Silica has two inherent disadvantages with respect to broad band SCG: low nonlinear refractive index and strong absorption beyond 2.5 μm wavelength.

Hence researchers have found switched over to nonsilica glasses developing devices operating in mid-IR region.ZBLAN (ZrF_4- BaF_2-LaF_3-AlF_3-NaF) glasses are used for generating continuum between ultraviolet to mid-IR region. Long fibers are required to

[2] The result of this chapter has been communicated to journal of ***Applied Optics***, June 2016.

generate broader spectrum since the nonlinear refractive index is comparable to that of silica, but has excellent transmission property beyond 2.5 μm wavelength. SC has been generated in IR and mid-IR range using ZBLAN fibers [65,66].

Tellurite fibers are also used for nonlinear applications. Tellurite has excellent transmission characteristics in near-IR and mid-IR range as shown in Fig 6.2. It has excellent chemical properties, high robustness, good thermal stability and offers strong resistance to corrosion [67]. It has a nonlinear refractive index which almost ten times of silica. These features have made tellurite an excellent candidate for SCG in mid-IR region. SC spanning upto 4.5 μm has been reported using an 8 mm long fiber [68].

Bismuth fibers have also been used for SCG. It has high nonlinear refractive index with good transparency in mid-IR region (<6 μm) [69-74]. Theoretically SC spanning upto 5 μm has been demonstrated [73]. Experimentally SC upto 3 μm has been obtained using micorstructured Bismuth fibers at a pump wavelength of 1.54 μm [74].

Chalcogenide glasses contain one or more elements from group 16 of the periodic table (S, Se, Te but excluding O) covalently bonded to networks formers such as As, Sb, Ge, Si etc [75]. These glasses have at least two orders higher nonlinear refractive index to that of silica glasses and an excellent IR and mid-IR transmission window upto 20 μm [76]. These two factors have made chalcogenide an excellent choice for fabricating mid-IR nonlinear photonic devices. The SCG in this region also covers most of the molecular fingerprint spectral region and is a natural choice for IR and mid-IR SCG [77]. A number of experimental and theoretical work on SCG has been carried out on chalcogenide waveguides [78-81] and fibers [82-87]. In the earlier reported works, the maximum broadening from 1.4 to 13.3 μm [85] and 2 to 15 μm [61] has been achieved using high peak power of 520 kW and 3.5 kW respectively. In the present design, a SCG spanning from 2-17 μm has been generated using a peak power of 3 kW.

7.2 Design and analysis:

The primary step in generation of SCG is to obtain zero dispersion at pump wavelength. To calculate dispersion, effective mode index of the structure at pump wavelength is to be determined. The effective mode index of the fundamental mode is calculated using full vectorial, finite element method (FEM) based software “COMSOL Multiphysics”. The

wavelength dependent refractive index or linear refractive index is calculated using selliemer's equation [88].

$$n(\lambda) = \sqrt{1 + \frac{A_1\lambda^2}{\lambda^2 - B_1^2} + \frac{A_2\lambda^2}{\lambda^2 - B_2^2}} \tag{7.1}$$

where, A_1= 5.78525, A_2=0.39705, B_1=0.28795, B_2=30.39338 and λ is the pump wavelength in micrometers.

The SCG is obtained by solving nonlinear Schrodinger wave equation described by Eqn 3.1. The nonlinear Schrodinger wave equation is a combination of linear and nonlinear terms. The linear terms include attenuation loss α and the dispersion parameter β. The attenuation loss α is taken as 0.6 dB/cm. The dispersion D is calculated using Eqn 7.1 which takes into account material dispersion. Using the effective mode index dispersion parameter upto n^{th} order is obtained solving Eqn. 3.5. The nonlinear coefficient γ is calculated using Eqn 3.3. The nonlinear coefficient n_2= 4.3 x 10^{-18} m^2/W at 3.1 μm [89]. The effective mode area is calculated using equation Eqn 3.4 . The Raman response is calculated Eqn 3.8. For $Ge_{11.5}As_{24}Se_{64.5}$ chalcogenide glass τ_1 =15.5 fs and life time τ_2=230.5 fs and f_R is 0.031 [93]. The simulation considers a secant hyperbolic pulse as described by Eqn 5.2.

The design consists of a $Ge_{11.5}As_{24}Se_{64.5}$ chalcogenide glass with three layers of air holes arranged in hexagonal lattice pattern as shown in Fig 7.1 (a).

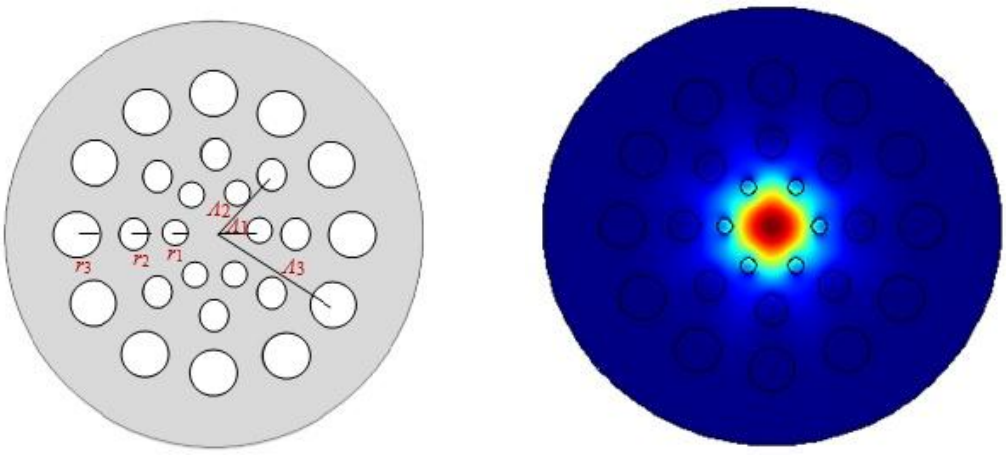

(a) (b)

Fig 7.1. (a) Transverse cross section of proposed HCGI PCF; (b) the electric field distribution of fundamental mode propagating in PCF at 2.8 μm wavelength

The x,y co-ordinates of the centre of the air hole is $x=\Lambda_n \cos\theta$, $y=\Lambda_n \sin\theta$ with n= 1,2,3 Λ_n is the distance of the center of the air hole from the axis of PCF, θ is the angle between subtended between x-axis and the line joining the axis of PCF to the center of air hole. The inner ring consists of six air holes at $\theta = 0^0, 60^0, 120^0, 180^0, 240^0, 300^0$. The middle ring consists of eight air holes at $\theta = 0^0, 45^0, 90^0, 135^0, 180^0, 225^0, 270^0, 315^0$. The outer ring consists of twelve air holes at $\theta = 0^0, 30^0, 60^0, 90^0, 120^0, 150^0, 180^0, 210^0, 240^0, 270^0, 300^0, 330^0$. The radius of inner, middle and outer ring are r_1, r_2, and r_3 respectively with $r_1 < r_2 < r_3$. The air filling fraction (r_n/Λ_n) increases gradually with the order of ring. In other words the effective refractive index of the cladding monotonically decreases, as we move outwards from the axis of the PCF and hence the structure is named as 'graded-index'. Hexagonal shaped core and graded index profile increases the confinement of the electric field and also results in a monotonically decreases refractive index profile. The proposed design has a strong control over dispersion profile and ZDWL. The simulated electric field of the fundamental mode propagating a 2.8 μm wavelength is shown in Fig. 1(b).

8.3 Dispersion Characteristics:

The variation of the six parameters Λ_1, Λ_2, Λ_3, r_1, r_2, and r_3 effects the dispersion profile of the proposed design. A thorough analysis by varying all the six parameters has been carried out and the design has been optimised to obtain minimum dispersion at pump wavelength of 2.8 μm with minimum effective mode area. The variation in dispersion characteristics due to variation in Λ_1 has been displayed in Fig 7.2 (a). The variation of position of inner ring of air hole Λ_1 has influenced the dispersion characteristics of the PCF. As the position of the inner ring of the air hole increased from the center, the effective mode area increases and ZDWL shifts towards shorter wavelength. The change in zero dispersion wavelength is small. In other words it can be infered that, zero dispersion wavelength can be controlled by controlling the position of the inner circle. The dispersion at 2.8 μm wavelength varied from -2.62 ps/nm km at Λ_1= 1.68 μm to -0.69 ps/nm km at Λ_1= 1.75 μm. For a variation of 0.02 μm in Λ_1 the dispersion varied by about 0.7 ps/nm km. The effective mode area varied from 5.30 μm^2 to 5.66 μm^2 as the position or Λ_1 was from 1.70 μm to 1.75 μm.

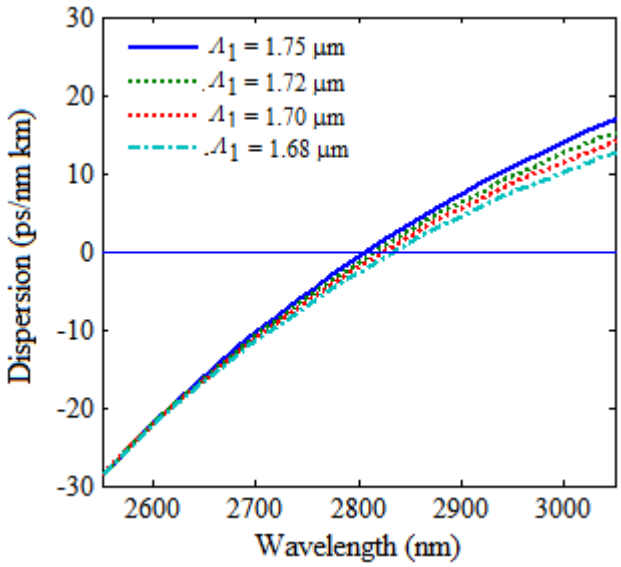

Fig 7.2 (a) Dispersion characterisitcs due to change in pitch of inner ring

The variation in dispersion characteristic due to variation in radius of air hole r_1 of inner ring has been displayed in Fig 7.2 (b). The influence of variation in radius of air hole on dispersion characteristics is higher compared to the changes in dispersion characteristics due to pitch of the air hole. This is due to reason that increase in radius of air hole increases the ratio of area of air hole to the area of chalcogenide, decreasing the effective refractive index. The change in refractive index due to variation in radius of air hole is much higher compared change in refractive index due to variation in position or pitch of the inner ring.

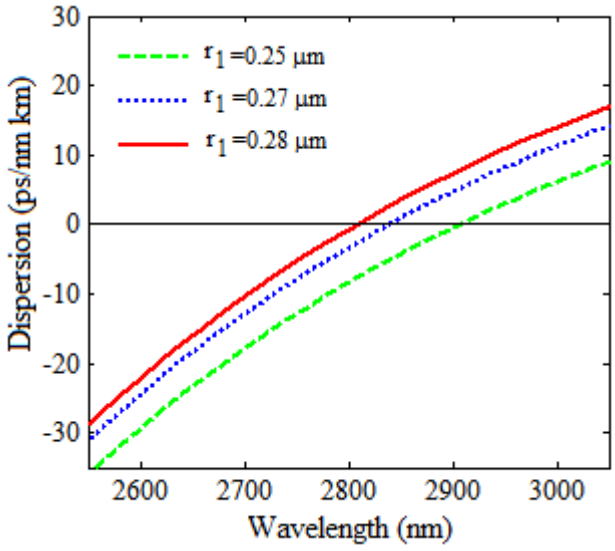

Fig 7.2 (b) Dispersion characterisitcs due to change in radius of air hole of inner ring

At 2.8 μm wavelength the dispersion at r_1=0.20 μm is -15.33 ps/nm km (not shown in the figure). The dispersion decreases to -8.37 ps/nm km as radius of air hole r_1 is increased to 0.25 μm and to -3.8 ps/nm km at r_1=0.27 μm. At r_1=0.28 μm the dispersion is -0.69 ps/nm km. The variation in radius has significant influence on dispersion characteristics. As the radius of the air hole is increased the ZDWL shifts towards longer wavelength. The effective mode area also decreases with increase in radius of the air hole. At r_1=0.25 μm the effective area is 5.88 μm^2, at r_1=0.27 effective mode area is 5.66 μm^2 and at r_1=0.28 μm the effective mode area is 5.56 μm^2.

The variation in position of second ring has lesser influence on effective mode index and effective mode area as compared to the variation of position due to inner ring as shown in Fig 7.3 (a). The position Λ_2 of the intermediate air hole ring has been varied between 2.48 μm to 2.52 μm in a step of 0.02 μm. The dispersion at Λ_2= 2.48 μm is 1.091 ps/nm km and dispersion at Λ_2= 2.52 μm is -2.422 ps/nm km. As the position of the air hole is increased the ZDWL shifted towards longer wavelength. The effective mode area increased from 5.52 μm^2 to 5.59 μm^2. The influence on dispersion due to variation of Λ_2 is higher compared to Λ_1.

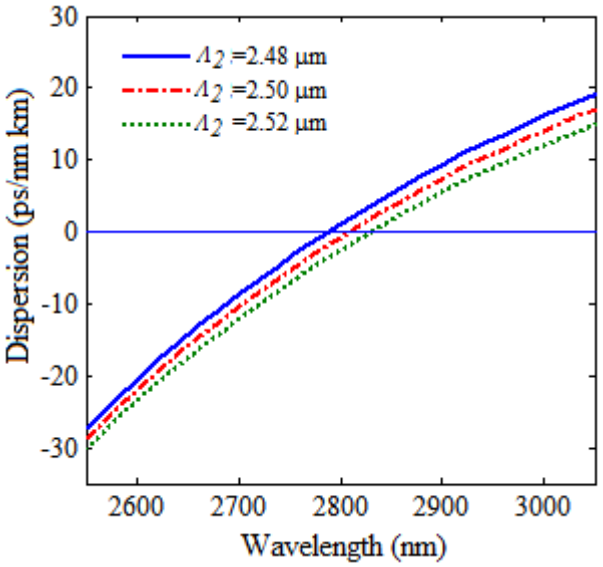

Fig 7.3 (a) Dispersion characterisitcs due to change in position of air hole of secondr ring

The variation in radius of intermediate air hole ring influences the ratio of area of air hole to the area of chalcogenide thus changing the overall refractive index of the structure. An increase in radius of air hole will lower the effective refractive index. The variation in dispersion characteristics of the structure due to variation in radius of the air hole of the

intermediate ring is shown in Fig 7.3(b). The radius of the air hole has been varied in steps of 0.02 μm.As the radius is increased the ZDWL shifts towards shorter wavelength. The dispersion at r_2=0.42 μm is 2.262 ps/nm km and dispersion at r_2=0.38 μm is -3.629. A change of radius by 0.02 μm varies the dispersion by approximately 2 ps/nm km. The effective mode area also increases from 5.51 μm^2 to 5.61 μm^2 as the radius is decreased from 0.42 μm to 0.38 μm.

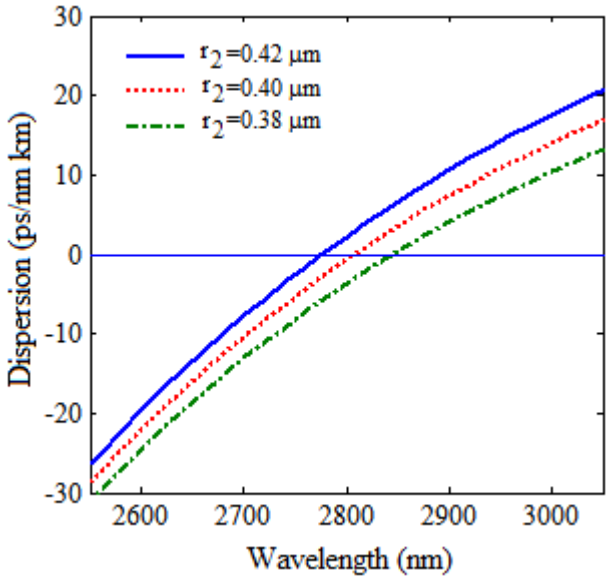

Fig 7.3 (b) Dispersion characterisitcs due to variation in radius of air hole of second ring

The variation in pitch or radius of third or outermost ring has very least influence on the dispersion characteristics of the proposed structure. The parameters of the third ring can be used for fine tuning the ZDWL since the variation in the parameters shifts the ZDWL by a very small value. The variation in dispersion characteristics due to variation in position of the third ring is shown in Fig 7.4 (a). The variation is minimal. The dispersion at 2.8 μm wavelength is -0.72 ps/nm km for Λ_3 = 3.92 μm and -0.60 ps/nm km for Λ_3 = 3.88 μm. For a variation of 0.04 μm the change in dispersion is about 0.1 ps/nm km. As the position of the third ring is moved away from the center the ZDWL shifts towards longer wavelength. There is no change in effective mode area.

The variation of dispersion in the proposed design due to variation in the radius r_3 of air hole of the third ring is shown in Fig 7.4 (b). The influence of the radius of the air hole of third ring on dispersion is minimum. The dispersion value at 2.8 μm wavelength for r_3= 0.58 μm is -0.6 ps/nm km and the dispersion value for r_3= 0.64 μm is -0.34 ps/nm km. The effective

mode area is at theses values are 5.56 μm^2 and 5.55 μm^2 respectively. As the radius of the airhole is increased the ZDWL shifts towards shorter wavelength.

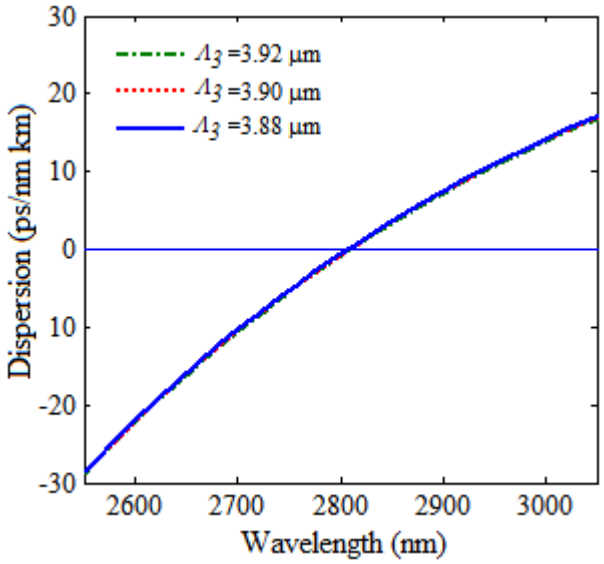

Fig 7.4 (a) Dispersion characterisitcs due to variation in position of air hole of third ring

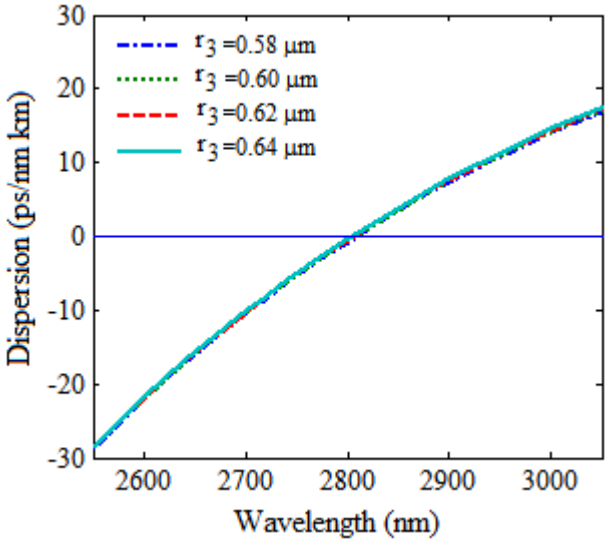

Fig 7.4 (b) Dispersion characterisitcs due to variation in radius of air hole of third ring

At Λ_1=1.75 μm, Λ_2 =2.50 μm, Λ_3 =3.80 μm, r_1 = 0.28 μm, r_2= 0.40 μm, and r_3=0.60 μm a dispersion of -0.6 ps/nm km has been obtained with an effective mode area 5.55 μm^2. The dispersion characteristics between 1 to 12 μm has been shown in Fig 7.5. The dispersion characteristics indicate that the structure has a very high dispersion value at shorter wavelength. The dispersion value near the pump wavelength is approximately zero. The structure has anomolous dispersion between 3 to 5 μm and normal dispersion between 5 to

12 μm. The maximum dispersion value in anomolous dispersion region is about 50 ps/nm km.

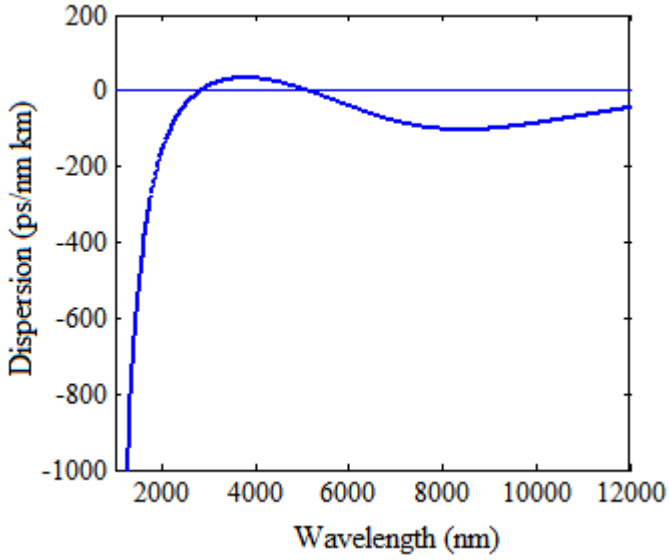

Fig 7.5 Dispersion characteristics of the proposed design

The variation of nonlinear coefficient γ and effective with respect to wavelength area is

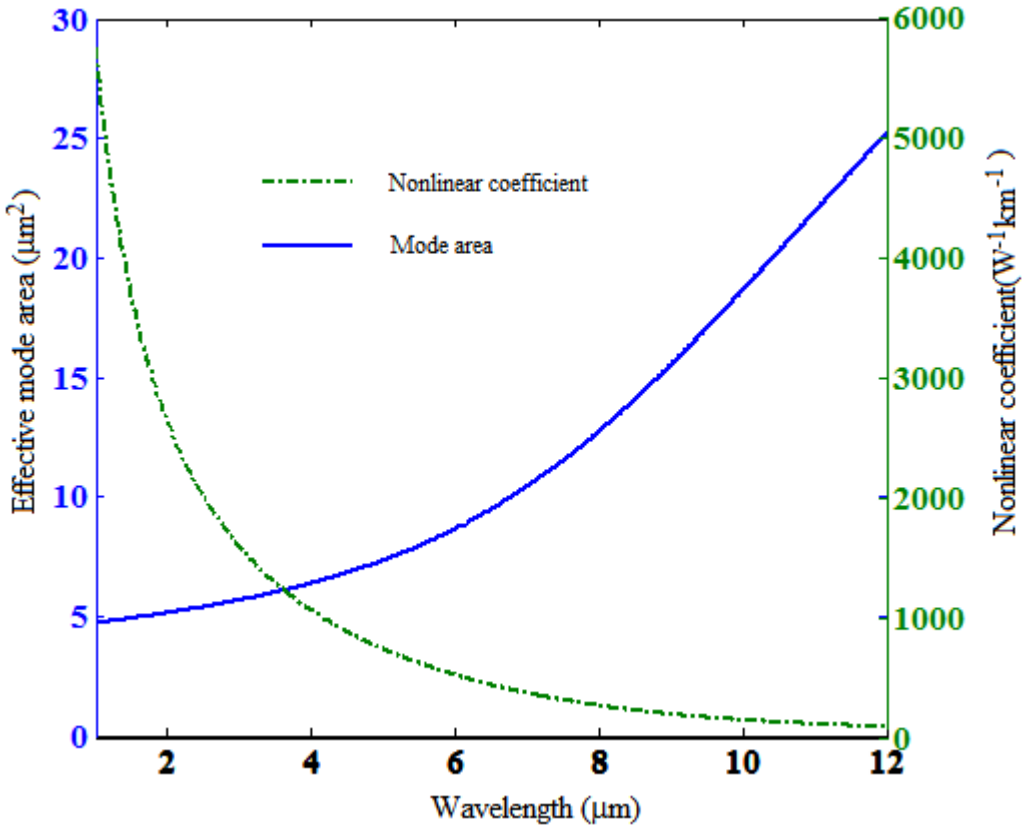

Fig 7.6 Variation of nonlinear coefficient and effective mode area against wavelength

shown in Fig 7.6. At shorter wavelength the effective mode area is small or confinement of fundamental mode inside the core is better. Therefore the effective mode area is small and as result the nonlinear coefficient is large. As the wavelength increases the effective mode area increases and hence the nonlinear coefficient decreases. The effective mode area at 2.8 μm wavelength is 5.55 μm^2 and confinement loss is 0.16 dB/mm. The nonlinear coefficient is calculated using equation Eqn 3.3 and is 1722 $W^{-1}km^{-1}$.

7.4 Supercontinuum generation:

The SCG has been generated by solving Eqn 3.1 using MATLAB. The influence of various parameters on the proposed design as discussed in section 3.3 has been studied. Influence of parameters like fiber length, pulse width and pulse power on SCG has been studied using MATLAB.

To study the effect of fiber length on SCG a secant hyperbolic pulse with a pulse width of 50 fs and peak power of 3000 W has been used for simulation and analysis. Spectrum has been obtained for various lengths of fiber from 0 mm to 12 mm in steps of 2 mm. At l= 0 mm the input pulse is shown in Fig 7.7. The pulse will not experience any change. This short duration high intensity pulse will initially undergo self-phase modulation as it starts propagates along the fiber. Along with self-phase modulation other nonlinear phenomenon also come into play and as a result spectral broadening occurs as evident at l=2mm. Since the dispersion is minimum at pump wavelength the shape of the pulse is undistorted leading to an efficient SPM. As the pulse further propagates more and more nonlinear phenomenon occur and the spectral width broadens as evident from at l= 4 mm, 6mm and 8 mm. At l= 10 mm the entire nonlinear process is complete, and a completely broadened spectrum is obtained. On further propagation the pulse will not broaden, instead will experience loss due to the fiber. Hence the optimum SCG is obtained at l= 10 mm. At l= 12 mm the spectrum has experienced higher losses due to material and the overall reduced spectral power. The extremely longer wavelength and extremely shorter wavelength will experience higher losses as the pulse propagates beyond the optimum length as is evident from the spectrum obtained at 12 mm.

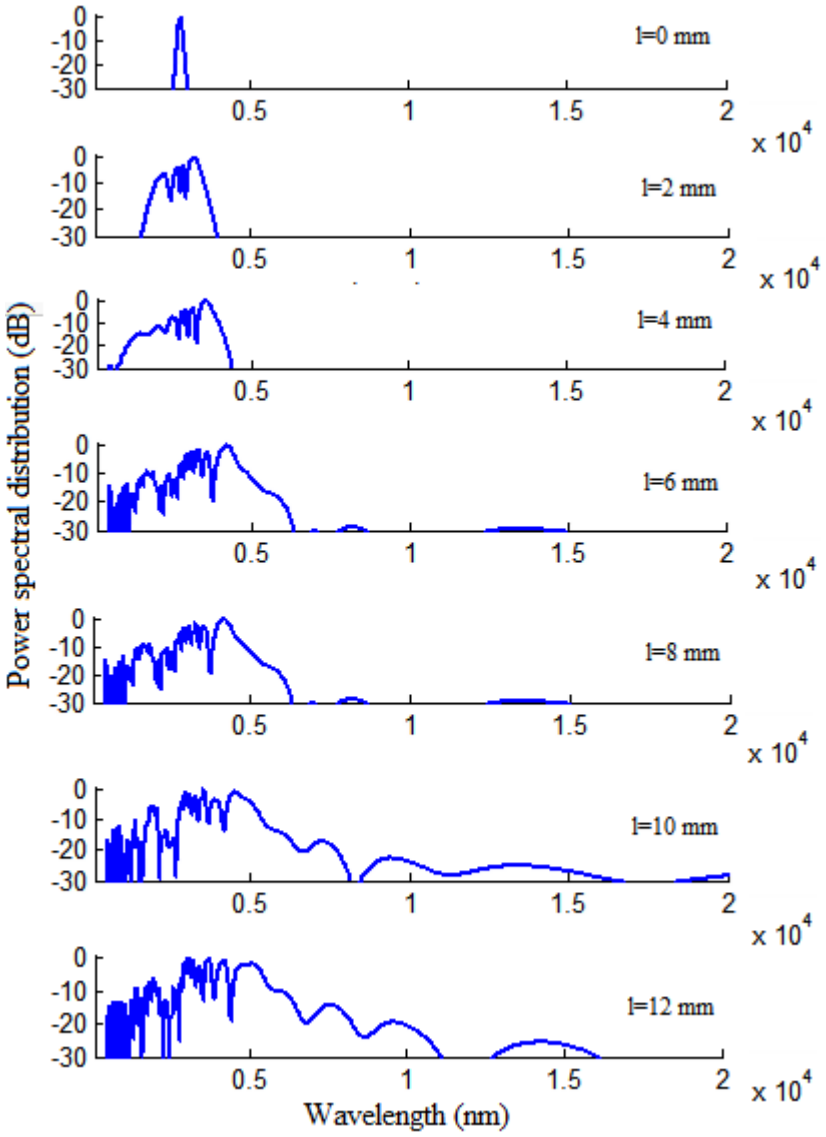

Fig 7.7 Influence of fiber length on SCG

The effect of variation in pulse width is studied using a fiber length of 10mm and pulse power of 3000 W. Secant hyperbolic pulse of pulse width varying from 50 fs to 200 fs increasing in steps of 50 fs has been simulated and spectrum has been obtained for these values as shown in Fig 7.8. At shorter pulse width, the rate of change of intensity is high and will result in an effective SPM. This will be followed by other nonlinear phenomenon like CPM, FWM and SRS. A broader continuum is obtained. As the pulse width is increased the rate of change of intensity reduces thus reducing the SPM. Thus the overall continuum broadening reduces. The continuum broadening has decreased as pulse width is increased from 50 fs to 100 fs. The spectrum has further reduced when the pulse width of the pulse launched is 150 fs.

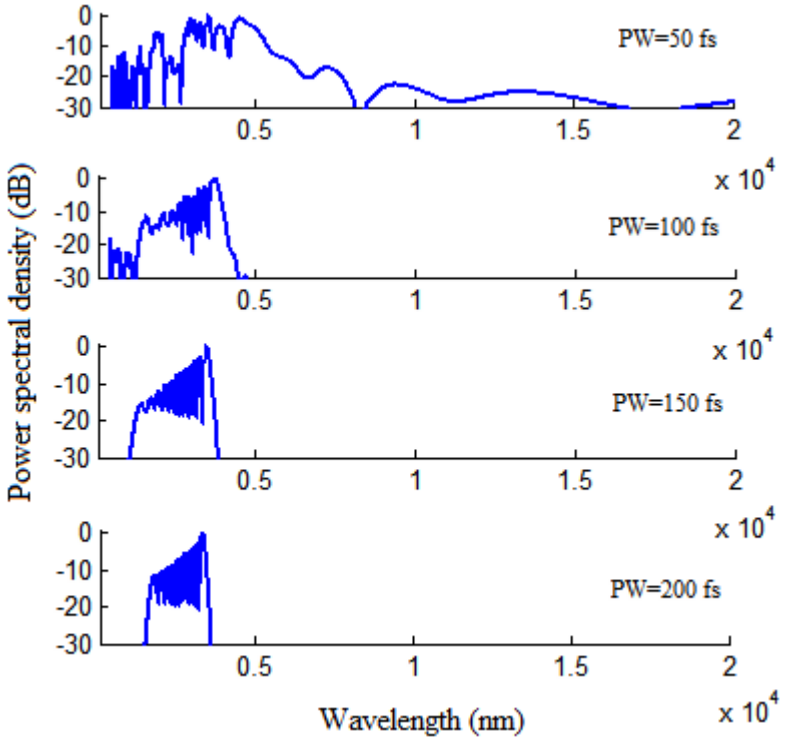

Fig 7.8 Influence of pulse width on SCG

In case a broader spectrum has to be obtained at larger pulse width then pulse should have higher peak power. The additional power will compensate for the decrease in rate of change of intensity.

The effect of variation of peak power of the pulse on SCG has been studied using a 10 mm Chalcogenide glass fiber with a secant shape pulse of pulse width 50 fs. The variation of spectrum with respect to pulse power has been shown in Fig 7.9. The peak power has been varied between 500 to 3500 W in steps of 500 W. When the power is low the intensity of the pulse is low. At low power the effect of SRS is limited and hence spectrum broadening is limited. As the power is increased the broadening also increases due to generation of stokes and anti-stokes wave. The broadening will increase only till a certain increase in power and further increase will have no influence on spectrum broadening. At higher power the spectrum will be much flat compared to that of spectrum obtained at low output. The increase in power will negate the losses experienced by the spectrum at the extreme long and short wavelength region.

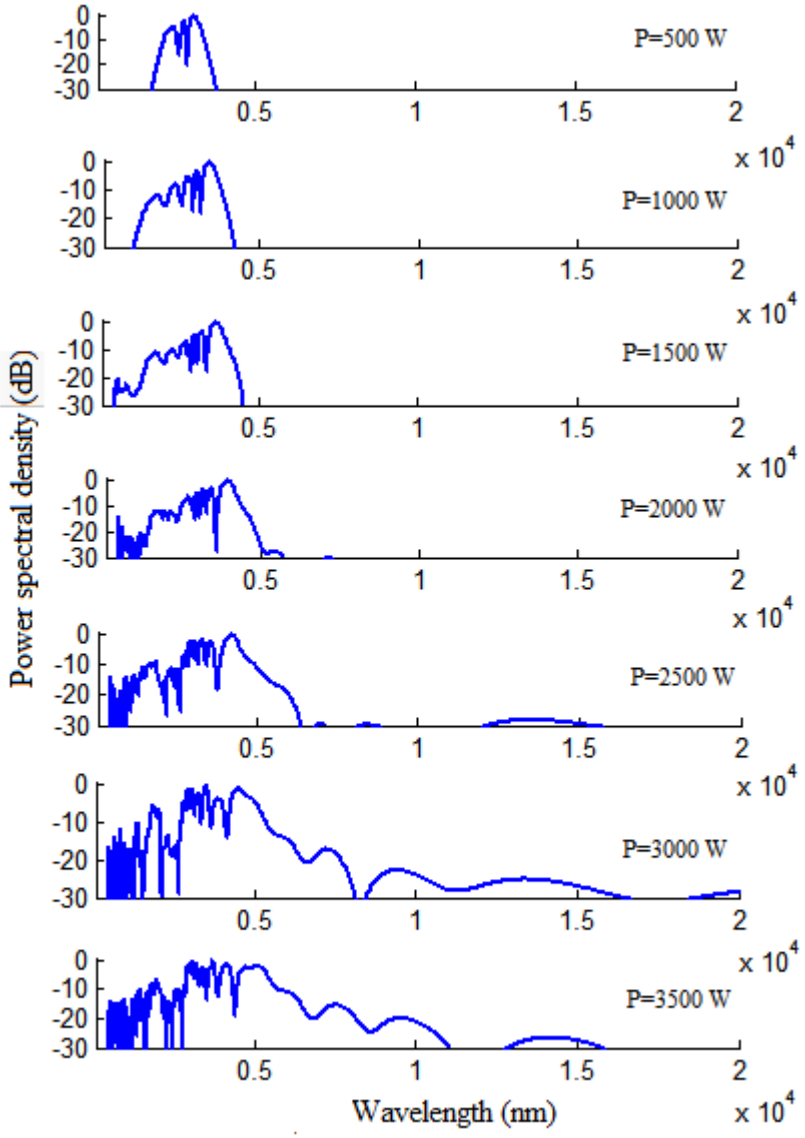

Fig 7.9 Effect of peak power on SCG

7.5 Conclusion:

A novel $Ge_{11.5}As_{24}Se_{64.5}$ based chalcogenide glass graded index photonic crystal fiber structure has been reported for mid-infrared super continuum generation. The proposed structure possesses a very high nonlinearity (γ=1722 $W^{-1}Km^{-1}$) at pump wavelength of 2.8 µm with very low and flat dispersion of -0.60 ps/nm km. A broadband spectrum spanning 1-16 µm using a 10 mm graded-index photonic crystal fiber with a peak power of 3 kW has been simulated. Such ultra-broadband supercontinuum spectrum is expected to have profound applications in various fields. The specific applications of mid-IR supercontinuum generation include spectroscopy, optical coherence tomography, frequency comb generation, early cancer detection, food quality control, security and sensing.

Chapter 8

Conclusions and scope for future work

8.1 Results and discussion:

Supercontinuum generation has been simulated in a coaxial multicore silica fiber, coaxial multicore tellurite fiber and chalcogenide glass graded index photonic crystal fiber. SCG for multicore fiber has been generated using RP fiber power software. SC for chalcogenide graded index PCF has been simulated using finite element based COMSOL Multiphysics and MATLAB. Coaxial multicore step index fiber has large effective mode area compared to that of PCF. Silica has the lowest nonlinear refractive index. A larger effective mode area and low nonlinear refractive index reduces the nonlinear coefficient. Hence to generate supercontinuum in silica fibers, long fibers are required with high pulse energy.

Supercontinuum at visible region has been generated using a coaxial multicore silica fiber using a pump wavelength of 660 nm. Silica fibers have been designed for zero dispersion at pump wavelength. A spectrum of about 900 nm broad has been obtained using a fiber of 1m length, a pulse energy of 1 nJ and a pulse width of 100 fs.

Supercontinuum generation at visible region has been generated using a coaxial multicore tellurite fibers using a pump wavelength of 660 nm. Tellurite has a higher nonlinear coefficient compared to silica. A broader spectrum can be obtained using a pulse of lower energy and shorter fiber length. A spectrum of 1100 nm broad has been obtained using a pulse energy of 0.1 nJ and a fiber length of 1 m.

SCG in a step index fiber is inefficient due to large effective mode area. The large mode area reduces the nonlinear coefficient thus leading to an inefficient SCG. Even dispersion engineering in step index fiber is difficult. Hence PCF's are used for nonlinear applications.

SCG has been simulated using a chalcogenide glass graded index PCF. The nonlinear coefficient of chalcogenide glass are high compared to silica and tellurite. Dispersion engineering can be carried out by varying the position and size of the air holes for the required pump wavelength. The effective mode area is less compared to that of step index fibers. The proposed structure has a very less effective area and a flat dispersion in mid-IR region. A broad continuum upto 16 μm has been obtained using a pulse power of 3000 W.

8.2 Scope for future work:

Super continuum generation has been generated using step index and PCF. The step index fiber can be designed to operate single mode and zero dispersion at pump wavelength. The PCF has to be designed for all normal dispersion. This can be carried out by varying the radius and position of the air holes. The effective mode area has to be reduced to increase nonlinear coefficient to obtain a broader and flat spectrum. An all normal dispersion and reduction in effective mode area and minimum dispersion at pump wavelength can be achieved by varying the position and radius of the air holes.

References.

[1]. John M. Senior "Optical Fiber Communication, Principle and Practice" Third Edition, Dorling Kindersley. 2010.

[2]. J.C. Knight, T.A. Birks, P.St. J.Russel, D.M. Atkin "All silica single-mode optical fibre with photonic crystal cladding" Opt. Lett. 21(19), (1996), 1547-1549.

[3]. R.F. Cregan, B.J. Mangan. J.C. Knight, T.A. Birks, P. St. J. Russel, P. J. Roberts, D.C. Allan " Single-mode photonic band gap guidance of light in air" Science 285(5433) (1999), 1537-1539.

[4]. V.V.R.K. Kumar, A.K George, W.H. Reeves, J.C. Knight, T.St. J. Russell, F.G. Omenetto, A.J. Taylor " Extruded soft glass photonic crystal fiber for ultrabroad supercontinuum generation", Opt. Express, 10(25), (2002), 1520-1525.

[5]. S. Mahnkopf, R. Marz, M. Kamp, H.D. Guang, F. Lelarge and A. Forchel, "Tunable photonic crystal coupled-cavitylaser", IEEE J. Quantum Electron, 40(9), (2004), 2027-2029.

[6]. K. Morishita and Y. Miyake, "Fabrication and resonance wavelengths of long-period gratings wirteen in a pure-silica photonic crystal fiber by the glass structure change", J. Lightwave Technol. 22(12), (2004), 2842-2846.

[7]. A. Cucinotta, F.Poli, and S.Selleri, " Design of erbium-doped triangular photonic-crystal-fiber-based amplifiers", IEEE Photonics Technol. Lett., 16(9), (2004), 2027-2029.

[8]. L. Tao, A.R. Zakharian, M. Fallahi, J.V. Moloney and M. Mansuripur " Multimode interference based photonic crystal waveguide power splitter", J. Lightwave Technol. 22(12), (2004), 2842-2846.

[9]. K.K. Chow, C. Shu, L Chinlon and A. Bjarklev, "Polarization-insensitive widely tunable wavelength converter based on four-wave mixing in a dispersion-flattened nonlinear photonic crystal fiber", IEEE Photonics Technol. Lett. 17(3), 2005, 624-626.

[10]. T. Niemi, L.H. Frandsen, K.K. Hede, A. Harpoth, P.I. Borel and M. Kristensen, "Wavelength division demultiplexing using photonic crystal waveguides", IEEE Photonics Lett. 18(1), 2006, 226-228.

[11]. S. Bong-Shik, T. Asano, Y. Akhane, Y. Tanaka and S. Noda, "Multichannel add/drop filter based on in-plane hetero photonic crystals", J. Lightwave Technol., 23(3), 2005, 1449-1455.

[12]. S.P. Singh and N. Singh 'Nonlinear Effects in Optical Fibers: Origin, Management and Applications' PIER 73, 2007, 249-275.

[13]. Robert W Boyd 'Nonlinear Optics' Third Edition, 2013

[14]. Govind P. Agrawal 'Nonlinear Fiber Optics' Fifth Edition, 2013

[15]. Stolen, R.H. and C. Lin, " Self-Phase modulation in silica optical fibers" Physical Review A, 17(4), 1978, 1448-1453.

[16]. Kikuchi N and S.Sasaki, "Analytical evaluation technique of self-phase modulation effect on the performance of cascaded optical amplifier", J. Lightwave Tech., 13, 1995, 868-878.

[17]. Kikuchi, N, K. Sekine and S. Sasaki, "Analysis of XPM effect on WDM transmission performance", Electron. Lett. 33, 1997, 653-654.

[18]. J. A. Armstrong, N. Bloembergen, J. Ducuing, and P. S. Pershan "Interactions between Light Waves in a Nonlinear Dielectric", Phys. Rev. 127, 1918 (1962).

[19]. Y. R. Shen, The Principles of Nonlinear Optics (Wiley, New York, 1984)

[20]. M. Schubertand B. Wilhelmi, Nonlinear Optics and Quantum Electronics (Wiley, New York, 1986).

[21]. P. N. Butcher and D. Cotter, Elements of Nonlinear Optics (Cambridge University Press, Cambridge, UK, 1990).

[22]. Shibata, N., R. P. Braun, and R. G. Waarts, "Phase-mismatch dependence of efficiency of wave generation through four-wave mixing in single-mode optical fiber," IEEE, Journal of Quantum Electron., 23(7), 1997, 1205–1210.

[23]. Lan, G.-L., P. K. Banerjee, and S. S. Mitra, "Raman scattering in optical fibers," J. of Raman Spectrosc., 11, 1981, 416–423.

[24]. S.P. Singh, R Gangwar and N. Singh "Progress In Electromagnetic Research", PIER 74, 2007, 379–405.

[25]. Shen, Y. R. and N. Bloembergen, "Theory of stimulated brillouin and raman scattering," Phys. Rev. A, 137, 1965, 1787–1805.

[26]. Lewis, S. A. E., S. V. Chernikov, and J. R. Taylor, "Temperature dependent gain and noise in fiber Raman amplifier," Opt. Lett., 24, 1999, 1823–1825.

[27]. F. DeMartini, C. H. Townes, T. K. Gustafson, and P. L. Kelley "Self-Steepening of Light Pulses" Phys. Rev. **164,** 1967, 312-314.

[28]. Weizhu Bao And Dieter Jaksch "An explicit unconditionally stable numerical Method for solving damped nonlinear Schrodinger equations with a focusing nonlinearity" SIAM, 41(4), 2003, 1406-1426.

[29]. J.A.C. Weideman and B.M. Herbst "Split Step methods for the solution of Nonlinear Schrodinger wave equation", SIAM, 23(3), 1986, 485-507.

[30]. V. Sinkin, R. Holzlohner, J. Zweck, and C. R. Menyuk, "Optimization of the split-step Fourier method in modeling optical-fiber communications systems," Journal of Lightwave Technology, 21, 2003, 61-68.

[31]. T.R. Taha and Wei Yu "Finite Difference methods for numerical simulations for 1+2 dimensional NLS type equations",

[32]. Ismail M.S., Alamri S.Z. "Highly accurate finite difference method for coupled nonlinear Schrodinger equation", International Journal of Computer Mathematics, 81, 2004, 333–351.

[33]. Zheng H.X., Yu D.Y. "Simulation of ultrashort laser pulse propagation in silica fibre by FDTD+", International Journal of Infrared and Millimeter Waves, 25, 2004, 799–807.

[34]. R. A. Fisher and W.K Bischel, "Numerical studies of the interplay between self phase modulation and dispersion for intense plane wave laser pulses," Journal of Appl. Phys. 46, 1975, 4921- 4934.

[35] M.J. Ablowitz and J.F. Ladik "A nonlinear difference scheme and inverse scattering", Stud. in Applied Mathematics 55, (1976), 213-229.

[36]. J.W. Cooley and J.W. Tukey "An algorithm for the machine calculation of complex Fourier series", Math. Comput. 19, 1965, 297-301.

[37]. Ajoy Ghatak and K.Thyagarajan 'Lasers-Fundamentals and Applications' Second Edition 2011.

[38]. R.R. Alfano and S.L. Shapiro "Emission in the region of 4000 to 7000Å via four-photon coupling in glass", Physical review letters 24, 584 (1970).

[39]. R.R. Alfano and S.L. Shapiro "Observation of self-phase modulation and small scale filaments in crystals and glasses" Physical review, Letters 24, 592 (1970).

[40]. K.Mori, H.Takara, S.Kawanishi, M.Saruwatari and T. Morioka" Flatly broadened supercontinuum spectrum in a dispersion decreasing fiber with convex dispersion profile" Electron. Lett. 33 (21), 1997, 1806-1808.

[41]. Halina Abramczyk 'Dispersion Phenomena in optical fibers', Technical University of Lodz, Poland

[42]. L.A. OStrovskii "Envelope shock waves",Sov,Phys. JETP 24, 1967,797-801.

[43]. V.I. Karpman "Self modulation of nonlinear plane waves in dispersive media", JETP Lett.6, 1967, 277-279.

[44] V.I. Bespalov and V.I. Talanov "Self-action of electromagnetic waves in cubic", JETP Lett. 3, 1966, 307-310.

[45]. M. J. Weber, D. Milam. and W. L. Smith, "Nonlinear refractive index of glasses and crystals", Opt. Eng. 17(5), 1978, 463-469.

[46]. R. H. Stolen, J. P. Gordon, W. J. Tomlinson, and H. A. Haus "Raman response function of silica-core fibers" JOSA, 6(6), 1989, 1159-1166.

[47]. KJ Blow, D Wood" Theoretical description of transient stimulated Raman scattering in optical fibers", , IEEE Journal of Quantum Electronics 25 (12), 1989, 2665-2673.

[48]. Mark E. Davis " Numerical methods and modelling for chemical engineers" , John Wiley and Sons, First Edition, 1984.

[49]. Mathew O. Sadiku "Numerical Techniques in electromagnetics" Second Edition, 2000.

[50]. R.Spano, J.V. Glan, P.Sanchis, A.Martinez, J.Marti and L.Pavesi " Group velocity dispersion in horizontal slot waveguides filled by Si nanocrystals", Proc IEEE Int. Conf. Group IV Photon, 2008, 314-316.

[51]. Ajoy Ghatak and K.Thyagarajan '*Introduction to Fiber Optics*' First Edition 1998.

[52]. Xian Feng, Jindan Shi, Martha Segura, Nicolas M White, Pradeesh Kannan, Xiangzhua Zhang, Wei H Loh '*Towards Water-Free Tellurite Glass Fiber for 2-5 μm Non-linear applications*' Fibers Vol 1, 2013.

[53]. Raouf A. H. El-Mallawany '*Tellurite Glasses Handbook Physical properties and data*' Second Edition 2011.

[54]. Sidek Aziz, Zaidan Abdul Wahab '*Optical Properties of ternary tellurite glasses*'.

[55]. T.S. Saini, Amira Bali, V.Dahiya, Ravindra Sinha "Design of equiangular spiral Photonic Crystal Fiber of supercontinuum generation at 1550 nm" Proc. of SPIE, 9200-920012, Sept 2014.

[56]. JM Dudley and J.R. Taylor "Ten years of nonlinear optics in photonic crystal fiber" Nat Photonics 5 (2011), 141-148.

[57]. K.M. Hillgsoe, T.V. Andersen, H.W. Paulsen, C.K. Widsen, K. Molmer, S Kading, R. Krishansen, K.P. Hansen and JJ Larsen " Supercontinuum generation in photonic crystal fiber with two zero dispersion wavelength", Opt. Exp 18(2004), 299-308.

[58]. J. Hu, C.R. Menyuk, L.B. Shaw, J.S. Sanghera and I.D. Aggarwal "Maximising bandwidth of supercontinuum generation in As_2Se_3 chalcogenide fibers" Opt. Exp. 18(3), 6722-6739 (2010).

[59]. I.D. Aggarwal and J.S. Sanghera, "Development and application of chalcogenide glass optic fiber at NRL", J.Opt. electron Adv Matter,(2002), 665-678 .

[60]. B. Dabas, R.K. Sinha "Design of highly birefringent chalcogenide glass PCF: a simplest design", Opt. Commun., 284 (2011), 1186–1191.

[61]. T.S. Saini, A. Kumar, R.K. Sinha "Triangular-core large-mode-area photonic crystal fiber with low bending loss for high power applications" Appl. Opt. 53 (2014), 7246–725.

[62]. H. Ademgil, S. Haxha "Highly nonlinear birefringent photonic crystal fiber", Opt. Commun., 282 (2009), 2831–2835.

[63]. S. Haxha, H. Ademgil "Novel design of photonic crystal fibers with low confinement losses, nearly zero ultra flattened chromatic dispersion, negative chromatic dispersion and improved effective mode area**",** Opt. Commun., 281 (2010), 278–286.

[64]. Than Singh Saini, Ajeet Kumar, Ravindra Kumar Sinha "Broadband Mid-Infrared Supercontinuum spectra spanning 2-15 μm using As_2Se_3 Chalcogenide glass Triangular-Core Graded-Index Photonic Crystal Fiber" J. Lightwave Technology, 33(2015), 18, 3914-3919 .

[65]. C.Xia, Z.Xu, M.N. Islam, F.L. Terry, Jr., M.J. Freeman, A.Zakel and J. Mauricio "10.5 W time-averaged power mid-IR supercontinuum generation extending beyond 4 μm with direct pulse pattern modulation", IEEE J.Sel. Top. Quantum Electron 15(2) (2009), 422-434.

[66]. G. Qin, X.Yan, C.Kito, M.Liao, C.Chaudhari, T. Suzuki and Y. Ohishi "Ultra broadband .supercontinuum generation fro ultraviolet to 6.28 μm in a fluoride fiber", Appl. Phy. Lett. 95(16)(2009), 161103.

[67]. J. S. Wang, E. M. Vogel, and E. Snitzer, "Tellurite glass: new candidate for fiber devices," Opt. Matter. 3(3) (1994), 187–203.

[68]. P. Domachuk, N. A. Wolchover, M. Cronin-Golomb, A. Wang, A. K. George, C. M. B. Cordeiro, J. C. Knight, and F. G. Omenetto, "Over 4000 nm bandwidth of mid-IR supercontinuum generation in sub-centimeter segments of highly nonlinear tellurite PCFs," Opt. Express 16(10) (2008), 7161–7168.

[69]. Ryszard Buczynski, Henry Bookey, Mariusz Klimczak, Dariusz Pysz, Ryszard Stepien, Tadeusz Martynkien, John E. McCarthy, Andrew J. Waddie , Ajoy K. Kar and Mohammad R. Taghizadeh "Two Octaves Supercontinuum Generation in Lead-Bismuth Glass Based Photonic Crystal Fiber", Materials 7(2014), 4568-4668.

[70]. J. Gopinath, H. Shen, H. Sotbayashi, E.Ippen, T. Hasegawa, T. NAgshima and N. Sugimoto, "Highly nonlinear Bismuth-oxide fiber for smooth supercontinuum generation at 1.5 micron", Opt. Express 12(23) 5697-5702.

[71]. G. Bramibilla, F. Koizumi, V. Finazzi and D.J. Richardson "Supercontinuum generation in tapered bismuth silicate fibres", Electron Lett 41(14) (2005), 795-797.

[72]. J.T. Gopinath, H.M. Shen, H. Sotobayashi, E.P. Ippen, T. Hasegawa, T. Naashima and N Sugimoto " Highly nonlinear bismuth-oxide fiber for supercontinuum generation and femtosecond pulse compression", J. Lightwave Technology 23(11) (2005), 3591-3596.

[73]. J.H.V Price, T.M. Monro, H.Ebendorff-Heidepriem, F.Poletti, P. Horak, V.Finazzi, J.Y.Y. Leong, P. Petropoulos, J.C. Glanagan, G.Brambilla,X.Feng and D.J. Richardson " Mid-IR supercontinuum generation from nonsilica microstructured optical fibers", IEEE J.Sel Top. Quantum Electron 13(3) (2007), 738-749.

[74]. R.Buczynski, H.T. Bookey, D Pysz, R. Stepien, I. Kujawa., J.e. McCarthy, A.J. Waddie, A.K. Kar and M.R. Taghizadeh "supercontinuum generation up to 2.5 μm in photonic crystal fiber made of lead-Bismuth-galate glass", Laser Phys. Lett. 7(9) (2010), 666-672.

[75]. Xin Gai, Ting Han, Amrita Prasad, Steve Madden, Duk-Yong, Choi, Rongping Wang, Douglas Bullas and Barry Luther-Davies " Progress in optical waveguides fabricated from chalcogenide glasses", Opt. Express 18 (2010), 26635-26646.

[76]. J.A. Savage "Infrared Optical Materials and their antireflection coating"(Adam Hilger, Bristol, 1985).

[77]. Chen Wei, Xiushan Zhu, Robert A Norwood, Feng Song and N. Peyghambarian " Numerical investigation on high power mid-infrared supercontinuum fiber lasers pumped at 3 μm", Opt. Exp. 21, (2013), 29488-29504.

[78]. X. Gai, D. Choi, S. Madden, Z. Yang, R. Wang, and B. Luther-Devies, "Supercontinuum generation in the mid-infrared from a dispersion engineered As2S3 glass rib waveguide," Opt. Lett. 37(2012), 3870–3872.

[79]. Y. Yu, X. Gai, T. Wang, P. Ma, R. Wang, Z. Yang, D. Choi, S. Madden, and B. Luther-Davies, "Mid-infrared supercontinuum generation in chalcogenides," Opt. Mater. Express 3(2013), 1075–1086.

[80]. Y. Yu, B. Zhang, X. Gai, P. Ma, D. Choi, Z. Yang, R. Wang, S. Debbarma, S. J. Madden, and B. Luther-Davies, "A broadband, quasi-continuous, mid-infrared supercontinuum generated in a chalcogenide glass waveguide," Laser Photon. Rev. 8(2014), 792–798.

[81]. H. Liang, P. Krogen, R. Grynko, O. Novak, C. L. Chang, G. J. Stein, D. Weerawarne, B. Shim, F. X. Kärtner, and K. H. Hong, "Threeoctave-spanning supercontinuum generation and sub-two-cycle self-compression of mid-infrared filaments in dielectrics," Opt. Lett. 40(2015), 1069–1072.

[82]. A. B. Salem, R. Cherif, and M. Zghal, "Tapered As_2S_3 chalcogenide photonic crystal fiber for broadband mid-infrared supercontinuum generation," in Frontiers in Optics 2011/Laser Science XXVII OSA Technical Digest (Optical Society of America, 2011), paper FMG 6

[83]. I. Kubat, C. R. Petersen, U. V. Møller, A. Seddon, T. Benson, L. Brilland, D. Mechin, P. M. Moselund, and O. Bang, "Thulium pumped mid-infrared 0.9–9 μm supercontinuum generation in concatenated fluoride and chalcogenide glass fibers," Opt. Express 22 (2014), 3959–3967 .

[84]. D. D. Hudson, M. Baudisch, D. Werdehausen, B. J. Eggleton, and J. Biegert, "1.9 octave supercontinuum generation in a As2S3 step-index fiber driven by mid-IR OPCPA," Opt. Lett. 39(2014), 5752–5755

[85]. C. R. Petersen, U. Møller, I. Kubat, B. Zhou, S. Dupont, J. Ramsay, T. Benson, S. Sujecki, M. Abdel-Moneim, Z. Tang, D. Furniss, A. Seddon, and O. Bang, "Mid-infrared supercontinuum covering the 1.4–13.3 μm molecular fingerprint region using ultra-high NA chalcogenide step-index fiber," Nat. Photonics 8(2014), 830–834.

[86]. U. Møller, Y. Yu, I. Kubat, C. R. Petersen, X. Gai, L. Brilland, D. Mechin, C. Caillaud, J. Troles, B. Luther-Davies, and O. Bang, "Multi-milliwatt mid-infrared supercontinuum generation in a suspended core chalcogenide fiber," Opt. Express 23(2015), 3282–3291 .

[87]. Y. Yu, X. Gai, C. Zhai, S. Qi, W. Guo, Z. Yang, R. Wang, D. Choi, S. Madden, and B. Luther-Davies, "1.8–10 μm mid-infrared supercontinuum generation in a step-index chalcogenide fiber using low peak pump power," Opt. Lett. 40(2015), 1081–1084.

[88]. M.R. Karim, BMA Rahman and G.P. Agrawal "Dispersion Engineered $Ge_{11.5}As_{24}Se_{64.5}$ nanowire for super continuum generation: A parametric study", Opt. Exp. 25 (2014), 31029-31040.

[89]. M.R. Karim, B.M.A Rahaman and Govind P Agrawal " Mid-infrared supercontinuum generation using dispersion engineered $Ge_{11.5}As_{24}Se_{64.5}$ Chalcogenide channel waveguide", Opt. Express 23(5) (2015), 6903-6914.